1

2

Transposable element landscape changes are buffered by RNA silencing in aging *Drosophila*

5

6

Nachen Yang[1], Satyam P. Srivastav[1,2†], Reazur Rahman[3†], Qicheng Ma[1†], Gargi Dayama[1], Madoka Chinen[4], Elissa P. Lei[4], Michael Rosbash[3], and Nelson C. Lau[1,5*]

1. Boston University School of Medicine, Department of Biochemistry
2. Current address: Department of Molecular Biology and Genetics, Cornell University, Ithaca, NY USA
3. Brandeis University, Department of Biology and Howard Hughes Medical Institute
4. Nuclear Organization and Gene Expression Section, NIDDK, NIH
5. Boston University Genome Science Institute

* Corresponding author: NCL: nclau@bu.edu
† These authors contributed equally to this study.

18
19

20

Running title: Fly aging and transposable element genomics.

22

Keywords: *Drosophila* aging, transposable elements, extra-chromosomal DNA, *PAF1*

24

25

ABSTRACT

Genetic mechanisms that repress transposable elements (TEs) in young animals decline during aging, as reflected by increased TE expression in aged animals. Does increased TE expression during aging lead to more genomic TE copies in older animals? To answer this question, we quantified TE Landscapes (TLs) via whole genome sequencing of young and aged *Drosophila* strains of wild-type and mutant backgrounds. We quantified TLs in whole flies and dissected brains and validated the feasibility of our approach in detecting new TE insertions in aging *Drosophila* genomes when natural defenses like RNA interference (RNAi) pathways are compromised. By also incorporating droplet digital PCR to validate genomic TE loads, we confirm TL changes can occur in a single lifespan of *Drosophila* when TEs are not suppressed. We also describe improved sequencing methods to quantify extra-chromosomal DNA circles (eccDNAs) in *Drosophila* as an additional source of TE copies that accumulate during aging. Lastly, to combat the natural progression of aging-associated TE expression, we show that knocking down *PAF1,* a conserved transcription elongation factor that antagonizes RNAi pathways*,* may bolster suppression of TEs during aging and extend lifespan. Our study suggests that RNAi mechanisms generally mitigate genomic TL expansion despite the increase in TE transcripts during aging.

2

1   **INTRODUCTION**

2   All animal genomes carry the genetic burden of a sizeable reservoir of parasitic

3   elements called transposons or transposable elements (TEs). This TE burden can

4   range from the extreme >70% proportion of the axolotl genome [1, 2] to >50% in the

5   human genome [3] to >10% in the *Drosophila melanogaster* genome [4, 5]. TEs are

6   selfish invaders of animal genomes with some potential for stimulating more rapid gene

7   regulatory innovations like serving as novel enhancers [6], but more frequently are

8   detrimental to animal fitness when they insert into and disrupt expression of important

9   genes [7]. Therefore, conserved chromatin regulation and RNA-interference (RNAi)

10   pathways must silence TEs to ensure fertility and animal health. However, these

11   genomic defense mechanisms also weaken during animal aging concomitant with

12   observable decreases in genomic integrity in aging cells. This phenomenon has been

13   articulated in the hypothesis of TEs impacting aging [8].

14   Initial support for this hypothesis in the model organism *D. melanogaster* came

15   from studies of TE expression increasing in aging flies [9-11, 12]. For example, mutants

16   in chromatin silencing factors and RNAi pathway genes which repress TEs have

17   reduced lifespans [9, 10, 13-16], whereas dietary restriction and overexpressing the

18   RNAi and chromatin factors can limit TE expression and promote longevity [13, 14].

19   Neurodegeneration modeled in aging flies through overexpressing aggregating proteins

20   like TDP-43 and TAU also leads to elevated TE expression [17-20]. Additionally, there

21   is evidence of a somatic population of Piwi proteins which can serve an additional TE

22   defense mechanism that when mutated leads to shorter lifespan and loss of stem cell

23   maintenance [13, 16, 21-23].

3

1   Beyond flies, mammals also must repress TEs for critical development of germ

2   cells, embryos and neurons. Mammals have a complex, interconnected network of

3   silencing pathways like the axis of SETDB1 [24, 25], KAP1 [26-28] and the HUSH

4   complex [29-32]; and its cooperation with histone deacetylases like SIRT6 [33, 34] and

5   histone methyltransferases like Suv39h1 and G9A [35-37]. In addition, there are DNA

6   methyltransferases that genetically interact with the piRNA pathway to target TEs for

7   chromatin silencing in mammalian germ cells [38-44]. In primates and mice, the most

8   active TE is the *LINE-L1* which is implicated in somatic genome mosaicism in

9   developing brains and individual neurons [45-53]. Lastly, *LINE-L1* is linked to

10   deleterious novel mutations in tumors and they are activated in cell culture models of

11   cellular senescence [54-59]. Although TE control is clearly important to mammalian

12   health, the large genome sizes and longer lifespans hampers comprehensive

13   assessments of mammalian TLs during impact aging.

14   Therefore, in this study we leveraged *Drosophila's* rapid aging, its compact

15   genome and powerful genetic tools as significant advantages for testing how TE

16   landscapes may change during normal animal aging. An important goal of our study is

17   to address the debate of whether TLs quantitated from Whole Genome Sequencing

18   (WGS) of *Drosophila* genomes represent true gains in TE genomic load [60]. One

19   bioinformatics program called TEMP [61] has been used extensively in determining TE

20   insertions from *Drosophila* WGS [62, 63] but its capacity to distinguish bona fide TE

21   insertions from potential library sequencing artifacts has been re-examined [60]. Noting

22   the high degree of variability in TE insertion calls from various bioinformatics programs

23   applied to *Drosophila* WGS data [64], we therefore developed our own program called

24   the Transposon Insertion & Depletion AnaLyzer (TIDAL) to identify the tremendous

4

1   diversity of TLs across various *Drosophila* strains [65]. TIDAL's increased specificity in

2   TE determinations comes from requiring sequencing reads mapping to both sides of

3   genomic locus flanking the TE insertion. This specificity was benchmarked against

4   genomic PCR tests [65], and TIDAL has characterized TLs in other *Drosophila* studies

5   of genetic factors regulating TE silencing [66, 67].

6   In this study, we demonstrate how WGS and extrachromosomal circular DNA

7   (eccDNA) sequencing of aged and young flies can report changes in TLs during fly

8   aging. Although TE RNA upregulation is a recurring phenotype of aging wild-type flies,

9   we show that major changes in the genomic TLs are generally suppressed by the RNAi

10   pathway because RNAi mutants allow TEs to expand their genomic DNA (gDNA) copy

11   numbers. We also demonstrate that tissue-specific (i.e. fly brain tissues) gDNA

12   sequencing can sensitize the detection of genomic TL changes; and eccDNA

13   accumulation during aging of the *ISO1* strain is an additional feature of the hypothesis

14   of TEs impacting animal aging. Lastly, we show that genetically boosting RNAi activity

15   in aged flies via knockdown of *PAF1* can suppress TE RNAs and extend longevity.

16   Together, these results demonstrate that the RNAi pathway buffers genomic alterations

17   by the natural increase of TE RNAs during aging and suggest *PAF1* inhibition in aging

18   animals could be a therapeutic target in this genetic mechanism of TE repression.

19

20   **RESULTS**

21   *Recurring increase of TE RNA expression during fly aging.*

22   Although previous studies using certain control wild-type (WT) fly strains showed

23   that TE RNAs were upregulated in aged flies [10, 14], we decided to reconfirm this

1   observation for three commonly used WT fly strains that would form the basis of this

2   study. Using our lab's standard rearing conditions, we first determined the aging curves

3   for the *ISO1* strain used for the *D. melanogaster* reference genome sequence [4], an

4   isogenic *w1118* strain that is a common background strain in genetic studies [68], and

5   the *Oregon-R* strain used in a series of functional genomics datasets [69]. Whereas

6   *w1118* and *OreR* displayed lifespans typical of other WT fly strains (**Figure 1A**), the

7   shorter lifespan of *ISO1* was expected because its genetic background was known to

8   sensitize phenotypes from chemical mutagenesis screens [70].

9   We then followed the experimental convention of other studies [10, 14] to

10   standardize the comparison of 30-day aged adults versus 5-day young adults, and we

11   performed quantitative RT-PCR on a panel of TEs from total RNAs from females (Fig.

12   1B). We replicated many examples of TE RNAs being upregulated in the aged WT flies

13   but noticed variability in which specific TE families were the most significantly

14   upregulated during aging. For example, *gypsy, mdg1,* and *I-element* were up regulated

15   at the RNA level in *ISO1* aged flies, while *copia* and *1731* RNAs were upregulated in

16   *w1118* and *OreR* (Fig. 1B). This variability may reflect the inherently distinct TLs

17   between these three strains [65], but the trend holds true that WT adult flies recurringly

18   experience increased TE expression during aging.

19   However, some previous studies examining *Drosophila* TEs during aging mainly

20   used a genetic reporter called the *gypsy-TRAP* to reflect increased transposition activity

21   in aging flies [13, 14, 18, 71]. This reporter has the advantage of low cost and sensitivity

22   of detecting small numbers of cells in a background of nonmodified cells, yet this

23   transgenic construct is also only designed for *gypsy* to insert and activate a fluorescent

24   protein read-out and cannot assess overall TLs. A newer and distinct TE activity

6

1   reporter called the *gypsy*-CLEVR puts the fluorescent protein expression cassette into

2   the domain of a 5X-UAS promoter only after retrotransposition, to take advantage of

3   cell-type or tissue specific GAL4 driver *Drosophila* strains [15]. Only one recent study

4   we are aware of assessed TLs during fly aging by WGS of enriched αβ-Kenyon Cell

5   neurons [60] and which argued that various pitfalls obscured the ability to observe TL

6   increases during fly aging. For example, the study itself discussed that Multiple

7   Displacement Amplification (MDA) required to amplify the minute amount of neuronal

8   gDNA prior to Illumina library construction could contribute to artifactual chimeric

9   molecules that represent false positive TE insertions [60]. Therefore, our more

10   comprehensive effort to examine TLs through direct WGS should add valuable insight to

11   this question.

12   First, some issues need to be considered in TL determinations in *Drosophila*

13   WGS datasets, such as two different TE-insertion discovery programs, TEMP [61] and

14   TIDAL [65] that each can yield different results from analyses of the same dataset

15   (**Figure S1**). Balancing sensitivity against specificity, TIDAL has similar trends as TEMP

16   in revealing the diversity of TLs amongst *Drosophila* samples (Fig. S1B) and both are

17   effective at calling germline insertions, but TIDAL avoids false positive predictions that

18   others have contended as somatic TE insertions (Fig. S1C, [60]). TIDAL handles this

19   issue differently by computing a Coverage Ratio (CR) score for each TE insertion from

20   pooled sequencing of a small group of flies (Fig. 1C), where TE insertion reads are

21   divided by reference genome mapping reads and a pseudocount of 1; such as a CR of

22   2 that we used as an arbitrary cutoff for indicating deep penetrance of a TE insertion at

23   a given insertion locus. When we re-analyzed the WGS datasets from [60] with TIDAL

7

1   even with the caveats of MDA, the TIDAL outputs do suggest increasing TLs within the

2   fly aging neuron genomes (**Figure S2**).

3

4   *Measuring TL differences by direct WGS and the TIDAL program.*

5   To meaningfully compare TL changes during a single generation of aging flies

6   from WGS and to avoid the genomic complications of normalizing against Y-

7   chromosome reads that are exceptionally dense with repeats [72], we only compared

8   samples from within the same strain in small numbers of young versus aged whole

9   female adult flies or female brains (Fig. 1D). In our process we extracted a set amount

10   of genomic DNA from 10 flies that allowed for reproducible WGS library construction

11   without requiring MDA or other total DNA amplification methods. We then sequenced on

12   the Illumina platform each fly strains' bulk gDNA library to a minimum >~30 million 75-

13   bp reads for >~16X fold genomic coverage of the version Dm6 genome assembly

14   (**Table S1**). Each library was analyzed identically with the TIDAL program [65] and new

15   TE insertions were counted individually and then normalized against the reads per

16   million measurement to account for sequencing depth differences. In developing our

17   own methodology to examine fly TLs during aging, we recall our previous study showing

18   that each fly strain's unique TLs depends on how inherently distinct its genetic

19   background is from the reference genome strain *ISO1* [65]. Therefore, it was expected

20   that new TE insertions quantified and normalized against each library's sequencing

21   depth would yield the lowest numbers for *ISO1* and the most TE insertion differences in

22   *w1118* and *OreR* (**Figure 2A**).

23   As expected, each of these WT flies TLs displayed completely distinct

24   compositions of new insertions of TE families relative to the Dm6 reference genome

1   sequence (Fig. 2B), such as a larger proportion of *hobo* TEs in *ISO1*, major infiltration of

2   *P-elements* in *OreR*, and several more *FB, pogo* and *412* TEs in *w1118*. Focusing on

3   the ratio of 30-day to 5-day insertions for the specific TE families making up the bulk of

4   these strains TLs, we could observe some increases in TE insertions in aged flies as

5   well as decreases (Fig. 2C). This was reflected at the total TL level with modest new TE

6   insertions in 30-day aged *ISO1* flies versus 5-day young flies, with also perplexing total

7   decreases in *OreR* and *w1118* flies (Fig. 2A). Although the vast majority of the TE

8   insertions were commonly detected by TIDAL in both 5-day and 30-day *w1118* and

9   *OreR* flies (Fig. 2D,E), there were more TE insertions only detected in these 5-day

10 young fly genomes than of 30-day aged flies. Only a few *hobo* insertions were also only

11 seen in 5-day young *ISO1* flies and were no longer detected in 30-day aged flies (Fig.

12 2). This observation can be explained by this analysis that only focuses on TE insertion

13 counts as quantile samplings of reads discordant from the reference genome. Thus, a

14 new somatic transposition event in a small subset of cells could be overshadowed by a

15 background of unmodified reference sequences and could explain a TE with a low CR

16 score that is sampled in 5-day fly gDNA sample but then missed in the 30-day sample.

17 This is a known limitation of the WGS approach and sacrificing sensitivity to improve

18 specificity in the original TIDAL program [65].

19   Therefore, we updated TIDAL to map to *Drosophila* TE families consensus

20 sequence coverage, and added arbitrarily-selected protein coding genes, analogous to

21 the modification to TEMP to track protein-coding genes as Immobile gene elements

22 (IGEs) [60]. We gauged a relatively low average rate (<4%, Table S1) of false positive

23 split reads called by TIDAL in hitting IGEs, whereas these protein coding genes

24 sequencing coverage generally also remained stable between 5-day young and 30-day

9

1   aged flies. (**Figure S3A**). Tracking TE consensus sequence coverage has the

2   advantage of accounting for all accumulating TE sequences in both the mappable and

3   unassembled and ambiguous-mapping regions of the genome. With this analysis

4   approach, we could detect a clearer increase of total TE sequence coverage in *OreR*

5   and *w1118* 30-day aged flies versus 5-day young flies (Fig. S3A). This overall aging-

6   associated increase in TE consensus sequence coverage was represented by many TE

7   families and is controlled against stable protein-coding gene coverage (Fig. S3B).

8   However, both this coverage analysis and the quantile insertions analysis cannot

9   discriminate between a full-length or truncated TE sequence, which we have noted in *P-*

10   *elements* can have critically variable transposition activities [73].

11

12   *Resolving and validating our approaches measuring TE landscapes with RNAi mutants.*

13   This unresolved genomics challenge of using short read WGS data for analyzing

14   TE sequences coverage also extends to some limitations in using droplet digital PCR

15   (ddPCR) to precisely quantify genomic TE copies for only the isoforms covered by the

16   short ddPCR amplicons [45]. Although the ddPCR quantifications of specific TE copies

17   (Fig. S3C) followed the similar proportional trends of TE families called by TIDAL (Fig.

18   2B), the aging-associated increases in TE copies measured by ddPCR in the WT fly

19   strains was also not detected. In questioning the accuracy of this ddPCR assay in

20   absolute quantification of TE copies, we compared ddPCR results on *P-elements* and *I-*

21   *elements* versus WGS and TIDAL determinations in two other directly matched gDNA

22   samples (**Figure S4A,B**). The ddPCR copy number measurements were very similar to

23   the WGS and TIDAL determinations, indicating both methodologies are consistent with

24   each other in the quantifications. Furthermore, we replicated a previously reported

10

1 genetic cross [74] that in one format triggers a large burst of *I-element* transposition in

2 the embryos but in a second format maintains *I-element* silencing (Fig. S4C). We

3 reanalyzed the WGS datasets from [74] with TIDAL reporting 505 new *I-element* copies

4 versus the 3732 insertions called by TEMP in that study, with our ddPCR results leaning

5 closer to the TIDAL count (1590 copies, Fig. S4D,E). These data reaffirm the findings

6 from [74] that the oocyte is the critical battleground between the host and the selfish

7 genetic element.

8 To explain why aging-associated TL changes seemed muted or were challenging

9 to detect in WT fly strains, we considered two competing hypotheses: (1) non-penetrant

10 TE insertions are masked by multiple unmodified genomic loci within the pools of

11 sequences imposing limitations in WGS and TIDAL analysis versus (2) WT flies retain

12 RNAi defenses like TE-targeting siRNAs [21, 22, 75-77] and piRNAs [13, 78-80] to

13 prevent increasing TE RNAs from completing genomic transposition events. To test

14 these hypotheses, we collected the same 5-day and 30-day aging cohorts from three

15 sets of different mutants in the two main arms of the RNAi pathway in *Drosophila*

16 (**Figure 3**). We analyzed two independent mutants each in the *piwi, aubergine, and*

17 *AGO2* genes and conducted the same whole flies WGS and TIDAL analysis as the WT

18 strains. In each of these six mutants, TLs showed dramatic increases in new TE

19 insertions during fly aging (Fig. 3A,B,C). There was still significant variability again in the

20 TLs between each mutant background, with no particular sets of TEs consistently

21 exhibiting increased transposition (Fig. 3D,E,F).

22 The ddPCR results above affirm that genomic approaches are capable of

23 detecting TL changes and WGS analysis of RNAi mutants demonstrate that the TL

11

1   changes can be detected during a single generation of aging flies. Therefore, we

2   conclude that although fly aging may allow TE RNAs to become upregulated [10, 13],

3   the RNAi pathways are still functioning in aging WT flies to mitigate TE RNAs from

4   transposing in genomes. In essence, the RNAi mutants raise the frequency of

5   successful TE mobilization events earlier in development so that these new insertions

6   become highly penetrant in the pooled population of the WGS libraries. This would also

7   suggest that successful TE insertions in WT flies are usually infrequent as to explain the

8   modest changes in WT TLs when sequencing genomes from whole flies.

9

10   *Detectable TL changes in fly brains during aging.*

11   Perhaps new TE insertions may be better detected in specific tissues were cells

12   that are more permanent and not turned over as frequently, such as the brain. For

13   example, in mammalian neurons, the most active TE *LINE-L1* has been implicated in

14   transposing relatively frequently during development to give rise to genomic mosaicism

15   in the brain [45-53]. Given the caveats of having to do prior total DNA amplification from

16   limited gDNA from fly neurons [60], we undertook WGS from at least 50 dissected

17   female brains to provide sufficient nucleic acid for RT-PCR confirmation of neuronal

18   gene expression and WGS of brain DNA (**Figure 4**).

19   We successfully generated libraries directly from brains of WT fly strains and *piwi*

20   and *AGO2* mutants without any prior total DNA amplification, and now we could detect

21   increases in TLs from *OreR* and *w1118* strains (Fig. 4B). Although there may be

22   piRNA-like small RNAs and *piwi* expression in fly heads [13, 21, 22], we detected

23   increases in TLs in *piwi* mutants' brains that were similar in magnitude to the WT *OreR*

12

1   and *w1118* strains (Fig. 4C). Greater and more variable increases in TLs were apparent

2   in the *AGO2* mutants' brains (Fig. 4D). Only the brains from the *ISO1* strain were

3   recalcitrant from showing much TE insertion increases except for a >2-fold increase in

4   the *Stalker* TE (Fig. 4B). Except for *ISO1*, the other fly strains appear to enable

5   increasing TL changes in the brain during fly aging.

6

7   *Extra-chromosomal circular DNAs (eccDNAs) as an additional genomic cache of*

8   *increasing TE sequences.*

9   In normal and diseased animal cells, there is a cache of eccDNAs that has

10 recently been explored by deep sequencing of DNA that is resistant to extensive

11 exonuclease digestion [81-84]. In certain tumor samples, eccDNAs are implicated in

12 rapid copy-number expansion of oncogenes [85], while ectopic accumulation of DNA in

13 the cytoplasm of senescing cells might trigger aging-associated inflammation responses

14 [86]. Several earlier studies had also found evidence of eccDNAs in *Drosophila*, with

15 the *copia* TE as a prominent example accumulating in certain strains [87-91]. Lastly,

16 eccDNA enriched in TE sequences and other repeats were detected in normal plants

17 and gDNA of human tissues [81, 92], which in both of these studies required total DNA

18 amplification prior to library construction to enrich the surviving eccDNAs after

19 exonuclease digestion.

20   We investigated eccDNAs in *Drosophila* by optimizing our own method to purify

21 enough eccDNAs to directly generate libraries for deep sequencing without requiring

22 prior total DNA amplification (**Figure 5A**). Furthermore, we used spike-ins of cloning-

23 vector plasmid DNAs into gDNA preparations and magnetic beads for improved

24 recovery and quantitation of eccDNAs for comparing between different samples. To

1   confirm that eccDNA was recovered after two rounds of Exo5 and Exo8 exonuclease

2   digestion steps which only degrade linear but not circular DNA, we conducted PCR with

3   standard primers amplifying linear genes and TEs (F1-R1 primer pairs, **Table S2**), and

4   outward-facing primers that either generate an amplicon from a TE eccDNA or tandem

5   genomic copies of the same TE (P10-P11 primer pairs) (Fig. 5B). Linear gene

6   amplicons were significantly depleted after exonuclease digestions, while the amplicon

7   for the spike-in plasmid was enriched. Linear TE amplicons were also reduced while

8   eccDNA-targeted amplicons for the *copia* TE was resilient against the exonuclease

9   treatment. Some other TE amplicons with outward-facing primers that were reduced

10 after exonuclease treatment may reflect more tandem copies of these TEs.

11   Since the regular PCR amplicons for the *copia* eccDNA were readily apparent in

12 WT strains (Fig. 5B), we used qPCR to quantify the changes and show that *copia*

13 eccDNA copies were increased >~2-fold in 30-day aged flies compared to 5-day young

14 flies (Fig. 5C). This result motivated us to deeply sequence short read libraries

15 generated directly from those eccDNA-enriched samples which did not undergo any

16 total DNA amplification (**Table S3**). We first adapted the TIDAL scripts of mapping reads

17 to the TE families consensus sequences to measure sequencing coverage as well as

18 circular junction spanning reads against *copia* and observed an aging-associated

19 increase in *copia* eccDNA that was consistent with our qPCR results (Fig. 5D). We also

20 applied this custom eccDNA quantitation pipeline to all the other *Drosophila* TEs as well

21 as adapting the CIRCLE-Map pipeline previously used to measure mammalian

22 eccDNAs [81] to the *Drosophila* TEs. We then normalized the ratios of the eccDNA-TE

23 counts between 30-day aged and 5-day young flies (Fig. 5E). Although the CIRCLE-

24 Map pipeline was more sophisticated at providing a significance "circle score" that we

14

1   set the cutoff to be >50, our custom eccDNA quantitation pipeline's results were notably

2   consistent in showing overall that most eccDNAs as TEs were increasing in the libraries

3   of 30-day aged flies (Fig, 5E, F). However, the additional normalization to the plasmid

4   spike-ins were more informative in moderating eccDNA levels in *w1118* while

5   reaffirming the TE eccDNA increases in *OreR* and *ISO1* (Fig, 5E, F). Thus, while *ISO1*

6   TLs did not change much at the chromosomal level during aging, *ISO1* TE copy

7   numbers may instead increase through eccDNA accumulation.

8

9   *Genetically enhancing RNAi counteracts TE expression during Drosophila aging*

10   Although TE expression still increased in WT aging flies, we hypothesized

11   whether endogenous RNAi pathways that still limit genomic TL increases could also be

12   genetically enhanced to mitigate the aging-associated rise of TE RNAs. To test this

13   hypothesis, we first used a ubiquitous *Tubulin-GAL4* driver to overexpress *AGO2* in

14   adults, and as expected, multiple TE RNAs had lowered expression relative to the

15   negative control (**Figure 6A**). We then used the same driver to overexpress *piwi,* and

16   although there was likely a silencing limit to prevalent *piwi* expression in the ovary, the

17   enhancement of *piwi* expression and TE silencing was much more apparent in the

18   female carcass (Fig. 6B).

19   These data provided a proof of principal that augmenting these RNAi pathways in

20   adults results in improvements in TE silencing. However, inhibiting a factor that

21   normally limits RNAi activity would be preferable from a therapeutic standpoint.

22   Examples of endogenous negative regulation of RNAi activity include proteasome-

23   mediated turnover of *AGO2* [93], ENRI factors that negatively regulate nuclear RNAi in

24   nematodes [94], and the RNA exosome and *PAF1*'s transcription elongation role

1   modulating RNAi silencing activity on TEs conserved in both fission yeast and flies [95-

2   97]. Even though we were able to use siRNA knockdown of *PAF1* in *Drosophila OSS*

3   cells to demonstrate enhanced TE silencing, we recognized that genetic knockdowns of

4   this essential modulator of RNAi would have detrimental effects on development like its

5   requirement in ovarian development [95].

6   So, to circumvent developmental impacts of *PAF1* knockdown in flies, we further

7   combined the temperature-sensitive inhibitor of GAL4 expressed from a second

8   transgene of *Tubulin-Gal80^ts* with the *Tubulin-Gal4* driver [98]. This double-transgenic fly

9   could then be crossed to the same UAS-*PAF1*-RNAi line so that flies can develop fully

10   at the permissive temperature of 18 °C, and after eclosion be raised at 29 °C to trigger

11   the RNAi knockdown of *PAF1* (Fig. 6C). Because elevated temperature itself can affect

12   TE silencing activity in flies [99-102], we used an *mCherry*-shRNA strain as a negative

13   control that was also raised at 29 °C at the same time as the *PAF1* knockdowns. There

14   was appreciable enhancement of TE silencing in the whole female flies at both 5-day

15   young and 30-day aged flies (Fig. 6C) with similar levels of TE silencing enhancement

16   between the ovaries and the soma (Fig. 6D). We attribute the increased TE silencing

17   during *PAF1* knockdown to the reduced elongation rate of TE transcripts so that RNAi

18   factors can better engage [95] and not from a global transcription reduction because

19   steady state levels of control gene, *TFIIs*, *AGO2* and *piwi* were not reduced by *PAF1*

20   knockdown (Fig. 6C,E).

21   Since we had observed TE landscape activity in the adult fly brain (Fig. 4), we

22   also tested a brain-specific driver, *elav-GAL4*, that was effective at triggering PAF1

23   knockdown and enhancing TE silencing in the 30-day aged fly brains (Fig. 6E).

24   However, this *elav-GAL4* driver that was likely reducing PAF1 levels in all neurons

16

1   during embryonic and adult development [103] also presented some problems like

2   reduced lifespan relative to the control, and we have not yet been able to recombine

3   *Tubulin-Gal80ts* with the *elav-GAL4* needed for the post-eclosion knockdown

4   experiment. Thus, we report the measured lifespans from the *PAF1* knockdown versus

5   the mCherry-shRNA negative control with the *Tubulin-Gal80^{ts}* and *Tubulin-Gal4* driver

6   cross at 29 ^{o}C (Fig. 6F). After an initial dip at 2 weeks, the *PAF1* RNAi knockdown flies

7   ended up living longer than the control and suggested that future pharmacological

8   inhibition of *PAF1* activity in maturing adult animals may be a relevant avenue of

9   intervening with the aging-associated increase in TE expression.

10

11   **DISCUSSION**

12   In this study we conducted an analysis of WGS approaches towards assessing

13   changing TLs during *Drosophila* aging, and we found that TL increases are readily

14   detectable in the genomes of aging RNAi mutants such as *piwi*, *aubergine* and *AGO2*.

15   These mutants are viable although others have shown that they have reduced longevity

16   compared to control strains [10, 13, 16], and our data now confirms that unchecked

17   elevation of TE transcripts can result in quantifiable genomic alterations in a single

18   lifetime of flies. However, it was more difficult to detect new TE insertions amongst the

19   gDNA of WT fly strains: we had to focus the TIDAL analyses on specific TE families

20   mobilizing into uniquely-mapping sequences and also count the coverage on TE family

21   consensus sequences (Fig. S3). After showing that an orthogonal quantitation method

22   like ddPCR is consistent with TIDAL's quantitation of TE copy numbers from WGS of *P-*

23   *elements* and *I-elements* (Fig. S4), our parsimonious conclusion is that despite aging-

17

1   associated increases in TE expression during fly aging, the RNAi pathway still protects

2   the fly genomes from massively accumulating new TE insertions.

3   Despite the compactness and completeness of the *D. melanogaster* genome

4   sequence, technical challenges still remain in fully optimizing WGS approaches to

5   quantify TLs. For example, all current metazoan genome assemblies still suffer from

6   large sequencing gaps in telomeric, centromeric and other repetitive regions that remain

7   unanalyzable. Meanwhile, long-read sequencing like Nanopore and PacBio that could

8   close these gaps are still less economical and not as accurate as the Illumina

9   sequencing platform [104], yet library construction methods for the Illumina platform

10   require sufficient input material for reproducible generation of sequencing libraries.

11   Single-cell WGS is not yet robust enough nor has total DNA amplification approaches

12   been demonstrated to be unhampered by molecule bias, so our study required pools of

13   genomes and non-amplified input DNA samples to reduce the prior concerns. Our study

14   also adds a second dimension to WGS of TLs by incorporating eccDNA as an *in vivo*

15   cache of accumulating TE DNA sequences (Fig. 5). Intriguingly, the *ISO1* strain showed

16   the least chromosomal TL changes yet exhibited the greatest increase in TE-eccDNAs

17   in the whole flies, while the *OreR* and *w1118* strains also showed evidence of TE-

18   eccDNAs accumulating in the brain (**Figure S5A**).

19   In addition to variations in TLs between WT strains, we also observed differences

20   in TLs between other RNAi mutants that we cannot fully explain. For example, we

21   examined aging-associated TLs from two EMS-induced point mutants of *Dcr-2*

22   *(L811fsx)* and *Dcr-2 (R416X)* from [105]), the nuclease acting upstream of *AGO2* to

23   generate the siRNAs from TE dsRNAs. However, there was inconsistent and contrary

24   TL differences between young and aged *Drosophila* in these *Dcr-2* mutants whole flies

18

1   and brains (Fig. S5B, C) as well as in *AGO3* mutants (Fig. S5D, [106]). Perhaps these

2   sets of mutants are not as penetrant in the loss of RNAi activity as the *piwi, aubergine*

3   *and AGO2* mutants. Furthermore, the analysis of a partially rescuing *AGO2* transgene

4   in the *AGO2 (2-5-14)* null mutant did lower the initial levels of TE insertion differences

5   noted by TIDAL, but the partial rescue still did not fully prevent aging-associated TE

6   increases (Fig. S5E), suggesting only wild type strength RNAi can buffer aging

7   genomes from accumulating new TE insertions.

8   Therefore, we propose that RNAi activity must be sustained during aging to

9   mitigate negative effects of increased TE expression in aged flies, a phenotype that has

10   also been frequently observed in mammals [34, 55, 107, 108]. To combat TEs' impact

11   on aging, some therapeutic approaches have used reverse transcriptase inhibitors and

12   drugs that inhibit *LINE-L1* activity [33], while other studies showed that dietary restriction

13   and prolonged exercise in animals can reduce aging-associated increases in TE

14   expression [14, 54, 109]. Our study proposes an additional therapeutic target of

15   augmenting the RNAi pathway's response to TEs by inhibiting *PAF1*, which has a

16   conserved impact on limiting RNAi from silencing TE transcripts [95, 96]. Perhaps

17   therapeutic siRNAs against *PAF1* transcripts can be hypothesized as a feed-forwarding

18   therapeutic agent to augment RNAi activity in aging animal cells.

19   A final question to resolve in the future is what cascade of epigenetic and

20   chromatin landscape changes during animal aging consistently leads to increases in TE

21   expression? Given the pleiotropic nature of the animal aging process, we anticipate

22   that there will also be multiple genomic mechanisms that will vary in impact between

23   different genetic backgrounds. For example, we describe variation amongst three WT

24   *Drosophila* strains in the level of accumulating eccDNAs containing TE sequences (Fig.

19

1   5), while others have shown increased in polyploidy in adult *Drosophila* brains [110] as

2   well as somatic genome instability in regions of the *Drosophila* genome [111] that might

3   contribute to changes at the level of TE consensus sequence coverages (Fig. S3B).

4   Lastly, during fly aging there are also gross-level changes in histone marks typically

5   associated with chromatin silencing [12, 14], which may precede the increase TE

6   expression, so the future extension of this work will be to add epigenetic and chromatin

7   accessibility landscapes to TLs during *Drosophila* aging.

8

9

10

11

12

1   **ACKNOWLEDGEMENTS**

12

13

14

15

MATERIALS AND METHODS

***Drosophila* strains, genetic crosses and aging curves**

All flies were raised at 25 °C on standard cornmeal food. For fly aging analyses, newly eclosed female flies were harvested from bottles and mated with males for two days. These females were then divided into ~20 individuals per vial and flipped to new vials every 2-3 days to mitigate crowding stress according to this protocol [112]. Surviving flies were counted at each flip, and the percentage of cumulative survival rate at each time point was plotted against its corresponding age (date of counting subtracted by date of eclosion).

The isogenized *ISO1* fly strain for the Dm6 reference genome sequence was obtained from Susan Celniker [4]; the *w1118* is an isogenized strain and was a gift from R. Scott Hawley [68]; and the *OreR* from the ModEncode project was a gift from Terry Orr-Weaver [69]. The RNAi pathway null mutant strains *piwi-(g1)*, *aubergine-(g1)*, *aubergine-(g2)*, *AGO3-(g1)* and *AGO3-(g2)* were a gift from Julius Brennecke [106]. An additional mutant strain of *Piwi-[HDR-4xP3-mCherry]* [113] was a gift from Eric Lai. The null *AGO2* mutants deletion strains of *AGO2-[2-5-14]* and *AGO2-[2-16-4]* and Ago2-WT-rescue stocks were generated by CRISPR Cas9 approaches as described in [114, 115]. The strains with active and inactive *I-elements* and spermless males were a gift from Zhao Zhang [74]. The UAS-Ago2-HA strain was a gift from Arno Muller lab [116] and the UASp-3xHA-Piwi was a gift from the Ruth Lehman lab [117]. The driver strains of *Tubulin-Gal4* and *elav*-Gal4 were a gift from Leslie Griffith [118]. In addition to a *Tubulin-Gal80^{ts}* strain we received from the Griffith lab, we also obtained a second *Tubulin-Gal80^{ts}* stock from the Bloomington *Drosophila* Stock Center (BDSC#7018) and combined with *Tubulin-Gal4* for further experiments. The *PAF1* knockdown RNAi line was obtained from the Vienna *Drosophila* Resource Center (VDRC#108826) and an mCherry shRNA control line was obtained from the Harvard TRiP resource (BDSC#35785).

To quantify *I-element* copies by ddPCR, fly cross schemes from [74] were replicated (Fig. S4C). Parental crosses between the w^{1118} strain with active *I-elements* and w^k strain with inactive *I-elements* were performed reciprocally to generate many virgin F1 females where one strain enables I-element transposition ("invaded" from w^k as the maternal parent) versus a control that maintains I-element silencing (w^{1118} as the maternal parent). These F1 females were then crossed to sperm-less males that were obtained as F1 male progenies from the parental cross of w^{1118} virgin females with XY attached male. F2 oocytes were collected overnight and DNA was extracted for ddPCR against the *I-element* and *Rp49*.

Fly brain isolation, genomic DNA extraction, WGS library construction and deep sequencing.

Fly brains were dissected from at least 50 females per age group, following a procedure laid out in [119]. Eye disks and other tissues were removed from heads with forceps, and brain lobes were dissected into tubes with ice-cold PBS before freezing once at -20 °C. Whole female flies and fly brains were homogenized in a standard DNA digestion buffer (1% SDS, 50 mM Tris-HCl pH 8.0, 100 mM EDTA, 100 mM NaCl, 0.5mg/ml Proteinase K) overnight at 50 °C, and then extracted using standard phenol chloroform extraction, ethanol precipitation, and resuspending gDNA pellets in pure water.

1   WGS of whole flies began with the circa 2014 Nextera Tn5 tagmentation kit (Illumina)
2 using an input of 50 ng gDNA and outputs were purified with AMpure XP beads (Beckman
3 Coulter). WGS libraries were quality controlled with the high-sensitivity DNA kit on the
4 Bioanalyzer (Agilent), selecting for size distributions of 300bp to 1kb and concentrations over 1
5 nM. Multiplexed libraries were sequenced on Illumina Nextseq500 high-output flow cells using
6 75 bp paired-end and single end kits. All WGS libraries were sequenced to a minimum depth of
7 35 million reads (Table S1, S2). After determining that some whole fly libraries made using
8 NEBNext Ultra-II DNA library prep kit for Illumina (NEB) were as complete and has better yields
9 than the then discontinued Nextera kit, we completed the fly brain gDNA libraries with the
10 NEBNext kit and sequenced them to similar depths as above.

11

12 **RNA extraction, quantitative RT-PCR, digital droplet PCR (dd-PCR) and TE copy number**
13 **estimation**
14   Total RNA was extracted from 5-10 female flies harvested at corresponding age with
15 TRI-reagent (MRC, Inc.). Reverse transcription (RT) was performed using random primers,
16 ProtoScript II (NEB), and 1 µg input of total RNA. Quantitative PCR (qPCR) with the Luna Sybr-
17 Green mastermix (NEB) used primer sequences in Table S3 and 2 µL of a 1:10 dilution of the
18 cDNA. Relative changes in gene expression were calculated using the $2^{\wedge}\Delta\Delta Ct$ method with
19 *Rp49* as a housekeeping gene for normalization.

20   Droplet digital PCR (ddPCR) was conducted on a QX200 instrument with the Evagreen
21 assay reaction (Biorad). Copy number measurements from specific TE primers (Table S3) were
22 normalized to *Rp49* as a diploid gene, starting first at 2 ng of gDNA as input per 20 µL ddPCR
23 for droplet generation for most TEs. For TEs with very high copy numbers that saturate the
24 droplets, input gDNA was diluted further to 2 ng into the ddPCR mix prior to droplet generation.
25 At least 10,000 droplets were required to achieve good statistical estimation of the concentration
26 calculated by Poisson distribution using Quantasoft Analysis Pro (Biorad). TE copy numbers per
27 genome was determined by dividing against half of the measured *Rp49* copies.

28 **Extracellular circular DNA isolation and sequencing**
29   To quantify eccDNAs during fly aging, 30 female flies were harvested from 5-days and
30 30-days post eclosion, and a fixed amount off pre-extraction plasmids was added prior to cell
31 lysis: ~80 pg of ~7kb-pGL3-DmPiwipro1 and ~50 pg of ~11kb-pCas9 prior to cell lysis. About 30
32 ug of total gDNA was recovered from using MasterPure™ Complete DNA and RNA Purification
33 kit (Lucigen), and 0.5ug-1ug gDNA was checked on a 1% agarose gel for integrity and quality.
34 Good gDNA primarily migrated at >10kb and to 20 µg gDNA we added 40ul of a second plasmid
35 cocktail: (1ng/ul of the 2.7kb pUC19, 0.1ng/ul of the 3.5kb pMaxGFP, 0.01ng/ul of the 5.2kb
36 pGSH0 and 0.001ng/ul of the 6.3kb pCENPm3) and split equally to two reactions: Exo5/8 non-
37 treated control versus Exo5/8 treated samples. We conducted a first round of Exo5/Exo8 (NEB)
38 treatment at 37 °C overnight, then an additional 2-hour treatment with freshly replenished buffer,
39 ATP and enzymes. The reaction was stopped and purified using AMPure XP beads (Beckman
40 Coulter) and eluted in 50 ul of water.

41   To check the efficiency of Exo5/8 treatment, 10 ul of the eluate from untreated versus
42 treated samples were loaded on 1% agarose gel to visualize complete digestion of gDNA. We
43 quality controlled Exo5/8 treatments by performing qPCR against rp49, ND5 and various

1   plasmid primers including pUC19, pGL3piwipro and pCas9 and Ct values were compared

2   between untreated versus treated samples. Mitochondria was not a reliable circular molecule

3   because of the high variability of ND5 Ct values across multiple sample preps. Comparing

4   between treated and untreated sample, the plasmids Ct values were generally stable (<2 Ct

5   difference), and much higher for rp49 (>5 Ct difference) indicating the Exo5/8 treatments were

6   effective at removing linear chromosomal DNA and not affecting the circular plasmids. Half of

7   the Exo5/8 treated sample (25 ul out of 50 ul purified elute) was used as template for library

8   construction using NEBNext UltraII library prep kit as stated above. Libraries were single end

9   (75bp) or pair-end sequenced at 36 bp by 36 bp on a Nextseq550 flow cell (Illumina).

10   For eccDNA sequencing from brains, 200 female brains were dissected and added with

11   half the volume of pre-extraction plasmids as whole flies, and gDNA concentration was

12   measured by the Qubit 4 Fluorometer (Thermofisher). To 100 ng of brain gDNA, we mixed 20 ul

13   of the plasmid spike-in cocktail and a tenth of the Exo5/8 enzyme as whole flies gDNA. At least

14   10 million eccDNA reads were required for analysis.

15   **TIDAL updates with total TE consensus and gene mapping strategies**

16

17   TE insertion analysis was carried out with an updated version of our previously

18   developed TIDAL program (original code available on the Github repository at:

19   https://github.com/laulabbrandeis/TIDAL) [65]. In this study, the updated version of TIDALv1.2 is

20   also posted to Github at (https://github.com/laulabbumc/TIDAL1.2). These scripts carry out the

21   analysis run the same way as the original TIDAL, but we incorporated two additional features.

22   First, for the euchromatic TE insertions we selected 22 arbitrarily selected protein coding gene

23   (Immobile gene elements IGEs) that are computed along with consensus TE sequence to

24   benchmark noise in detection of genetic elements. The algorithm used to identify transposon

25   insertion sites based on consensus transposon sequence is then applied on these 100 IGE

26   sequence to determine their insertion sites. Second, for the total reads mapped to consensus

27   TE sequences, here we added 100 IGEs are computed by mapping reads with bowtie2 using

28   parameters "--sensitive --end-to-end" and custom shell, Perl, C-code, and R-code scripts all

29   accessible from (https://github.com/laulabbumc/TIDAL1.2).

30

31   TEMP v1.05 code was acquired from the GitHub repository at:

32   (https://github.com/JialiUMassWengLab/TEMP), and was run with default parameters except "-

33   x 30, -m 3 -f 500". These parameters were chosen to ensure that TEMP results are consistent

34   with analysis shown in [60, 62].

35   **Bioinformatics counting of eccDNA from TEs and spike-in plasmids using a custom**

36   **pipeline and CIRCLE-Map program.**

37   In our first look at the eccDNA reads, we inputted them into an existing bioinformatics

38   pipeline already developed for mapping *Drosophila* small RNA counts to TEs [120]. Reads were

39   first checked by the Cutadapt program to see if adaptor sequences at the 3' end needed to be

40   removed, and then we indexed the reads to the *Drosophila* genome assembly file by running

41   BWA version 1 [121] and formatdb from NCBI. Using Bowtie1 with 2 mismatches [122], reads

42   were mapped to genome to get the genic and intergenic counts using the genome GTF file. The

43   total number of reads mapped to the *Drosophila* genome was derived by subtracting the total

1 number of reads not mapped to the *Drosophila* genome from the total number of

2 reads. The total number of mapped reads was used as the basis for normalization of TE counts

3 and spike-in plasmid counts.

4 Plasmid sequences were treated as linear entries in the FASTA file database similar to

5 the TE family consensus sequences. The raw read counts from TE mapping were further

6 normalized by the total number of reads mapping to the *Drosophila* Dm6 genome assembly. For

7 spike-in plasmid counting, because several plasmids share the same backbone with different

8 inserts, read frequencies were normalized by the total plasmid mapping sites as well as by the

9 total number of *Drosophila* genome-mapping reads.

10 To execute the CIRCLE-Map program for repeats [81], we indexed the *Drosophila*

11 genome FASTA file by BWA. We then used the MEM algorithm under BWA to align reads

12 against the *Drosophila* genome FASTA file. Next, we sorted the reads by alignment position

13 within the resulting BAM file and indexed the resulting BAM file. Finally, we detected the circles

14 by calling CIRCLE-Map program. The CIRCLE-Map program for repeats yields an output for

15 reads with two high scoring alignments as these ones are indicative of circles formed from

16 regions with homology.

17

18

19

20

21

25

REFERENCES

1.   Smith JJ, Timoshevskaya N, Timoshevskiy VA, Keinath MC, Hardy D, Voss SR. A chromosome-scale assembly of the axolotl genome. Genome research. 2019;29(2):317-24. Epub 2019/01/27. doi: 10.1101/gr.241901.118. PubMed PMID: 30679309; PubMed Central PMCID: PMCPMC6360810.

2.   Nowoshilow S, Schloissnig S, Fei JF, Dahl A, Pang AWC, Pippel M, et al. The axolotl genome and the evolution of key tissue formation regulators. Nature. 2018;554(7690):50-5. Epub 2018/01/25. doi: 10.1038/nature25458. PubMed PMID: 29364872.

3.   Lander ES, Linton LM, Birren B, Nusbaum C, Zody MC, Baldwin J, et al. Initial sequencing and analysis of the human genome. Nature. 2001;409(6822):860-921. doi: 10.1038/35057062. PubMed PMID: 11237011.

4.   Adams MD, Celniker SE, Holt RA, Evans CA, Gocayne JD, Amanatides PG, et al. The genome sequence of Drosophila melanogaster. Science. 2000;287(5461):2185-95. PubMed PMID: 10731132.

5.   Kaminker JS, Bergman CM, Kronmiller B, Carlson J, Svirskas R, Patel S, et al. The transposable elements of the Drosophila melanogaster euchromatin: a genomics perspective. Genome biology. 2002;3(12):RESEARCH0084. PubMed PMID: 12537573; PubMed Central PMCID: PMC151186.

6.   Chuong EB, Elde NC, Feschotte C. Regulatory activities of transposable elements: from conflicts to benefits. Nature reviews Genetics. 2017;18(2):71-86. doi: 10.1038/nrg.2016.139. PubMed PMID: 27867194; PubMed Central PMCID: PMCPMC5498291.

7.   Wells JN, Feschotte C. A Field Guide to Eukaryotic Transposable Elements. Annual review of genetics. 2020. Epub 2020/09/22. doi: 10.1146/annurev-genet-040620-022145. PubMed PMID: 32955944.

8.   Gorbunova V, Boeke JD, Helfand SL, Sedivy JM. Human Genomics. Sleeping dogs of the genome. Science. 2014;346(6214):1187-8. doi: 10.1126/science.aaa3177. PubMed PMID: 25477445; PubMed Central PMCID: PMC4312280.

9.   Chen H, Zheng X, Xiao D, Zheng Y. Age-associated de-repression of retrotransposons in the Drosophila fat body, its potential cause and consequence. Aging Cell. 2016;15(3):542-52. Epub 2016/04/14. doi: 10.1111/acel.12465. PubMed PMID: 27072046; PubMed Central PMCID: PMCPMC4854910.

10.   Li W, Prazak L, Chatterjee N, Gruninger S, Krug L, Theodorou D, et al. Activation of transposable elements during aging and neuronal decline in Drosophila. Nature neuroscience. 2013;16(5):529-31. doi: 10.1038/nn.3368. PubMed PMID: 23563579; PubMed Central PMCID: PMC3821974.

11.   Wood JG, Helfand SL. Chromatin structure and transposable elements in organismal aging. Frontiers in genetics. 2013;4:274. doi: 10.3389/fgene.2013.00274. PubMed PMID: 24363663; PubMed Central PMCID: PMC3849598.

12.   Wood JG, Hillenmeyer S, Lawrence C, Chang C, Hosier S, Lightfoot W, et al. Chromatin remodeling in the aging genome of Drosophila. Aging Cell. 2010;9(6):971-8. doi: 10.1111/j.1474-9726.2010.00624.x. PubMed PMID: 20961390; PubMed Central PMCID: PMC2980570.

13.   Jones BC, Wood JG, Chang C, Tam AD, Franklin MJ, Siegel ER, et al. A somatic piRNA pathway in the Drosophila fat body ensures metabolic homeostasis and normal lifespan. Nature communications. 2016;7:13856. doi: 10.1038/ncomms13856. PubMed PMID: 28000665; PubMed Central PMCID: PMCPMC5187580.

14.   Wood JG, Jones BC, Jiang N, Chang C, Hosier S, Wickremesinghe P, et al. Chromatin-modifying genetic interventions suppress age-associated transposable element activation and extend life span in Drosophila. Proceedings of the National Academy of Sciences of the United States of America. 2016;113(40):11277-82. doi: 10.1073/pnas.1604621113. PubMed PMID: 27621458; PubMed Central PMCID: PMCPMC5056045.

15.	Chang YH, Keegan RM, Prazak L, Dubnau J. Cellular labeling of endogenous retrovirus replication (CLEVR) reveals de novo insertions of the gypsy retrotransposable element in cell culture and in both neurons and glial cells of aging fruit flies. PLoS biology. 2019;17(5):e3000278. Epub 2019/05/17. doi: 10.1371/journal.pbio.3000278. PubMed PMID: 31095565; PubMed Central PMCID: PMCPMC6541305.

16.	Sousa-Victor P, Ayyaz A, Hayashi R, Qi Y, Madden DT, Lunyak VV, et al. Piwi Is Required to Limit Exhaustion of Aging Somatic Stem Cells. Cell reports. 2017;20(11):2527-37. Epub 2017/09/14. doi: 10.1016/j.celrep.2017.08.059. PubMed PMID: 28903034; PubMed Central PMCID: PMCPMC5901960.

17.	Chang YH, Dubnau J. The Gypsy Endogenous Retrovirus Drives Non-Cell-Autonomous Propagation in a Drosophila TDP-43 Model of Neurodegeneration. Curr Biol. 2019;29(19):3135-52 e4. Epub 2019/09/10. doi: 10.1016/j.cub.2019.07.071. PubMed PMID: 31495585; PubMed Central PMCID: PMCPMC6783360.

18.	Krug L, Chatterjee N, Borges-Monroy R, Hearn S, Liao WW, Morrill K, et al. Retrotransposon activation contributes to neurodegeneration in a Drosophila TDP-43 model of ALS. PLoS genetics. 2017;13(3):e1006635. doi: 10.1371/journal.pgen.1006635. PubMed PMID: 28301478; PubMed Central PMCID: PMCPMC5354250.

19.	Sun W, Samimi H, Gamez M, Zare H, Frost B. Pathogenic tau-induced piRNA depletion promotes neuronal death through transposable element dysregulation in neurodegenerative tauopathies. Nature neuroscience. 2018;21(8):1038-48. Epub 2018/07/25. doi: 10.1038/s41593-018-0194-1. PubMed PMID: 30038280; PubMed Central PMCID: PMCPMC6095477.

20.	Guo C, Jeong HH, Hsieh YC, Klein HU, Bennett DA, De Jager PL, et al. Tau Activates Transposable Elements in Alzheimer's Disease. Cell reports. 2018;23(10):2874-80. Epub 2018/06/07. doi: 10.1016/j.celrep.2018.05.004. PubMed PMID: 29874575; PubMed Central PMCID: PMCPMC6181645.

21.	Mirkovic-Hosle M, Forstemann K. Transposon defense by endo-siRNAs, piRNAs and somatic pilRNAs in Drosophila: contributions of Loqs-PD and R2D2. PloS one. 2014;9(1):e84994. Epub 2014/01/24. doi: 10.1371/journal.pone.0084994. PubMed PMID: 24454776; PubMed Central PMCID: PMCPMC3890300.

22.	Ghildiyal M, Seitz H, Horwich MD, Li C, Du T, Lee S, et al. Endogenous siRNAs derived from transposons and mRNAs in Drosophila somatic cells. Science. 2008;320(5879):1077-81. Epub 2008/04/12. doi: 1157396 [pii]

10.1126/science.1157396. PubMed PMID: 18403677.

23.	Lin KY, Wang WD, Lin CH, Rastegari E, Su YH, Chang YT, et al. Piwi reduction in the aged niche eliminates germline stem cells via Toll-GSK3 signaling. Nature communications. 2020;11(1):3147. Epub 2020/06/21. doi: 10.1038/s41467-020-16858-6. PubMed PMID: 32561720; PubMed Central PMCID: PMCPMC7305233.

24.	Kato M, Takemoto K, Shinkai Y. A somatic role for the histone methyltransferase Setdb1 in endogenous retrovirus silencing. Nature communications. 2018;9(1):1683. Epub 2018/04/29. doi: 10.1038/s41467-018-04132-9. PubMed PMID: 29703894; PubMed Central PMCID: PMCPMC5923290.

25.	Matsui T, Leung D, Miyashita H, Maksakova IA, Miyachi H, Kimura H, et al. Proviral silencing in embryonic stem cells requires the histone methyltransferase ESET. Nature. 2010;464(7290):927-31. Epub 2010/02/19. doi: 10.1038/nature08858. PubMed PMID: 20164836.

26.	Ecco G, Cassano M, Kauzlaric A, Duc J, Coluccio A, Offner S, et al. Transposable Elements and Their KRAB-ZFP Controllers Regulate Gene Expression in Adult Tissues. Developmental cell. 2016;36(6):611-23. Epub 2016/03/24. doi: 10.1016/j.devcel.2016.02.024. PubMed PMID: 27003935; PubMed Central PMCID: PMCPMC4896391.

27.	Rowe HM, Jakobsson J, Mesnard D, Rougemont J, Reynard S, Aktas T, et al. KAP1 controls endogenous retroviruses in embryonic stem cells. Nature. 2010;463(7278):237-40. Epub 2010/01/16. doi: 10.1038/nature08674. PubMed PMID: 20075919.

28.	Castro-Diaz N, Ecco G, Coluccio A, Kapopoulou A, Yazdanpanah B, Friedli M, et al. Evolutionarily dynamic L1 regulation in embryonic stem cells. Genes & development. 2014;28(13):1397-409. Epub 2014/06/19. doi: 10.1101/gad.241661.114. PubMed PMID: 24939876; PubMed Central PMCID: PMCPMC4083085.

29.	Tunbak H, Enriquez-Gasca R, Tie CHC, Gould PA, Mlcochova P, Gupta RK, et al. The HUSH complex is a gatekeeper of type I interferon through epigenetic regulation of LINE-1s. Nature communications. 2020;11(1):5387. Epub 2020/11/05. doi: 10.1038/s41467-020-19170-5. PubMed PMID: 33144593; PubMed Central PMCID: PMCPMC7609715.

30.	Robbez-Masson L, Tie CHC, Conde L, Tunbak H, Husovsky C, Tchasovnikarova IA, et al. The HUSH complex cooperates with TRIM28 to repress young retrotransposons and new genes. Genome research. 2018;28(6):836-45. Epub 2018/05/08. doi: 10.1101/gr.228171.117. PubMed PMID: 29728366; PubMed Central PMCID: PMCPMC5991525.

31.	Liu N, Lee CH, Swigut T, Grow E, Gu B, Bassik MC, et al. Selective silencing of euchromatic L1s revealed by genome-wide screens for L1 regulators. Nature. 2018;553(7687):228-32. Epub 2017/12/07. doi: 10.1038/nature25179. PubMed PMID: 29211708; PubMed Central PMCID: PMCPMC5774979.

32.	Tchasovnikarova IA, Timms RT, Matheson NJ, Wals K, Antrobus R, Gottgens B, et al. GENE SILENCING. Epigenetic silencing by the HUSH complex mediates position-effect variegation in human cells. Science. 2015;348(6242):1481-5. Epub 2015/05/30. doi: 10.1126/science.aaa7227. PubMed PMID: 26022416; PubMed Central PMCID: PMCPMC4487827.

33.	Simon M, Van Meter M, Ablaeva J, Ke Z, Gonzalez RS, Taguchi T, et al. LINE1 Derepression in Aged Wild-Type and SIRT6-Deficient Mice Drives Inflammation. Cell metabolism. 2019;29(4):871-85 e5. Epub 2019/03/12. doi: 10.1016/j.cmet.2019.02.014. PubMed PMID: 30853213; PubMed Central PMCID: PMCPMC6449196.

34.	Van Meter M, Kashyap M, Rezazadeh S, Geneva AJ, Morello TD, Seluanov A, et al. SIRT6 represses LINE1 retrotransposons by ribosylating KAP1 but this repression fails with stress and age. Nature communications. 2014;5:5011. doi: 10.1038/ncomms6011. PubMed PMID: 25247314; PubMed Central PMCID: PMCPMC4185372.

35.	Bulut-Karslioglu A, De La Rosa-Velazquez IA, Ramirez F, Barenboim M, Onishi-Seebacher M, Arand J, et al. Suv39h-dependent H3K9me3 marks intact retrotransposons and silences LINE elements in mouse embryonic stem cells. Molecular cell. 2014;55(2):277-90. Epub 2014/07/02. doi: 10.1016/j.molcel.2014.05.029. PubMed PMID: 24981170.

36.	Leung DC, Dong KB, Maksakova IA, Goyal P, Appanah R, Lee S, et al. Lysine methyltransferase G9a is required for de novo DNA methylation and the establishment, but not the maintenance, of proviral silencing. Proceedings of the National Academy of Sciences of the United States of America. 2011;108(14):5718-23. Epub 2011/03/24. doi: 10.1073/pnas.1014660108. PubMed PMID: 21427230; PubMed Central PMCID: PMCPMC3078371.

37.	Vogel MJ, Guelen L, de Wit E, Peric-Hupkes D, Loden M, Talhout W, et al. Human heterochromatin proteins form large domains containing KRAB-ZNF genes. Genome research. 2006;16(12):1493-504. Epub 2006/10/14. doi: 10.1101/gr.5391806. PubMed PMID: 17038565; PubMed Central PMCID: PMCPMC1665633.

38.	Schopp T, Zoch A, Berrens RV, Auchynnikava T, Kabayama Y, Vasiliauskaite L, et al. TEX15 is an essential executor of MIWI2-directed transposon DNA methylation and silencing. Nature communications. 2020;11(1):3739. Epub 2020/07/29. doi: 10.1038/s41467-020-17372-5. PubMed PMID: 32719317; PubMed Central PMCID: PMCPMC7385494.

39.	Zoch A, Auchynnikava T, Berrens RV, Kabayama Y, Schopp T, Heep M, et al. SPOCD1 is an essential executor of piRNA-directed de novo DNA methylation. Nature. 2020;584(7822):635-9. Epub 2020/07/17. doi: 10.1038/s41586-020-2557-5. PubMed PMID: 32674113.

40.   Carmell MA, Girard A, van de Kant HJ, Bourc'his D, Bestor TH, de Rooij DG, et al. MIWI2 Is Essential for Spermatogenesis and Repression of Transposons in the Mouse Male Germline. Developmental cell. 2007. PubMed PMID: 17395546.

41.   Kuramochi-Miyagawa S, Watanabe T, Gotoh K, Totoki Y, Toyoda A, Ikawa M, et al. DNA methylation of retrotransposon genes is regulated by Piwi family members MILI and MIWI2 in murine fetal testes. Genes & development. 2008;22(7):908-17. Epub 2008/04/03. doi: 22/7/908 [pii]

10.1101/gad.1640708. PubMed PMID: 18381894; PubMed Central PMCID: PMC2279202.

42.   Shoji M, Tanaka T, Hosokawa M, Reuter M, Stark A, Kato Y, et al. The TDRD9-MIWI2 complex is essential for piRNA-mediated retrotransposon silencing in the mouse male germline. Developmental cell. 2009;17(6):775-87. Epub 2010/01/12. doi: S1534-5807(09)00434-1 [pii]

10.1016/j.devcel.2009.10.012. PubMed PMID: 20059948.

43.   Zamudio N, Barau J, Teissandier A, Walter M, Borsos M, Servant N, et al. DNA methylation restrains transposons from adopting a chromatin signature permissive for meiotic recombination. Genes & development. 2015;29(12):1256-70. Epub 2015/06/26. doi: 10.1101/gad.257840.114. PubMed PMID: 26109049; PubMed Central PMCID: PMCPMC4495397.

44.   Pastor WA, Stroud H, Nee K, Liu W, Pezic D, Manakov S, et al. MORC1 represses transposable elements in the mouse male germline. Nature communications. 2014;5:5795. Epub 2014/12/17. doi: 10.1038/ncomms6795. PubMed PMID: 25503965; PubMed Central PMCID: PMCPMC4268658.

45.   Bedrosian TA, Quayle C, Novaresi N, Gage FH. Early life experience drives structural variation of neural genomes in mice. Science. 2018;359(6382):1395-9. doi: 10.1126/science.aah3378. PubMed PMID: 29567711.

46.   Erwin JA, Paquola AC, Singer T, Gallina I, Novotny M, Quayle C, et al. L1-associated genomic regions are deleted in somatic cells of the healthy human brain. Nature neuroscience. 2016;19(12):1583-91. doi: 10.1038/nn.4388. PubMed PMID: 27618310; PubMed Central PMCID: PMCPMC5127747.

47.   Marchetto MC, Narvaiza I, Denli AM, Benner C, Lazzarini TA, Nathanson JL, et al. Differential L1 regulation in pluripotent stem cells of humans and apes. Nature. 2013;503(7477):525-9. doi: 10.1038/nature12686. PubMed PMID: 24153179.

48.   Muotri AR, Chu VT, Marchetto MC, Deng W, Moran JV, Gage FH. Somatic mosaicism in neuronal precursor cells mediated by L1 retrotransposition. Nature. 2005;435(7044):903-10. doi: 10.1038/nature03663. PubMed PMID: 15959507.

49.   Richardson SR, Gerdes P, Gerhardt DJ, Sanchez-Luque FJ, Bodea GO, Munoz-Lopez M, et al. Heritable L1 retrotransposition in the mouse primordial germline and early embryo. Genome research. 2017;27(8):1395-405. doi: 10.1101/gr.219022.116. PubMed PMID: 28483779; PubMed Central PMCID: PMCPMC5538555.

50.   Baillie JK, Barnett MW, Upton KR, Gerhardt DJ, Richmond TA, De Sapio F, et al. Somatic retrotransposition alters the genetic landscape of the human brain. Nature. 2011;479(7374):534-7. doi: 10.1038/nature10531. PubMed PMID: 22037309; PubMed Central PMCID: PMC3224101.

51.   Evrony GD, Lee E, Park PJ, Walsh CA. Resolving rates of mutation in the brain using single-neuron genomics. eLife. 2016;5. doi: 10.7554/eLife.12966. PubMed PMID: 26901440; PubMed Central PMCID: PMCPMC4805530.

52.   Evrony GD, Lee E, Mehta BK, Benjamini Y, Johnson RM, Cai X, et al. Cell lineage analysis in human brain using endogenous retroelements. Neuron. 2015;85(1):49-59. doi: 10.1016/j.neuron.2014.12.028. PubMed PMID: 25569347; PubMed Central PMCID: PMCPMC4299461.

53.   Poduri A, Evrony GD, Cai X, Walsh CA. Somatic mutation, genomic variation, and neurological disease. Science. 2013;341(6141):1237758. doi: 10.1126/science.1237758. PubMed PMID: 23828942; PubMed Central PMCID: PMC3909954.

1 54.   De Cecco M, Criscione SW, Peterson AL, Neretti N, Sedivy JM, Kreiling JA. Transposable elements
2 become active and mobile in the genomes of aging mammalian somatic tissues. Aging (Albany NY).
3 2013;5(12):867-83. doi: 10.18632/aging.100621. PubMed PMID: 24323947; PubMed Central PMCID:
4 PMCPMC3883704.
5 55.   De Cecco M, Criscione SW, Peckham EJ, Hillenmeyer S, Hamm EA, Manivannan J, et al. Genomes
6 of replicatively senescent cells undergo global epigenetic changes leading to gene silencing and
7 activation of transposable elements. Aging Cell. 2013;12(2):247-56. doi: 10.1111/acel.12047. PubMed
8 PMID: 23360310; PubMed Central PMCID: PMCPMC3618682.
9 56.   De Cecco M, Ito T, Petrashen AP, Elias AE, Skvir NJ, Criscione SW, et al. L1 drives IFN in senescent
10 cells and promotes age-associated inflammation. Nature. 2019;566(7742):73-8. Epub 2019/02/08. doi:
11 10.1038/s41586-018-0784-9. PubMed PMID: 30728521; PubMed Central PMCID: PMCPMC6519963.
12 57.   deHaro D, Kines KJ, Sokolowski M, Dauchy RT, Streva VA, Hill SM, et al. Regulation of L1
13 expression and retrotransposition by melatonin and its receptor: implications for cancer risk associated
14 with light exposure at night. Nucleic acids research. 2014;42(12):7694-707. Epub 2014/06/11. doi:
15 10.1093/nar/gku503. PubMed PMID: 24914052; PubMed Central PMCID: PMCPMC4081101.
16 58.   Rodic N, Sharma R, Sharma R, Zampella J, Dai L, Taylor MS, et al. Long interspersed element-1
17 protein expression is a hallmark of many human cancers. Am J Pathol. 2014;184(5):1280-6. Epub
18 2014/03/13. doi: 10.1016/j.ajpath.2014.01.007. PubMed PMID: 24607009; PubMed Central PMCID:
19 PMCPMC4005969.
20 59.   Huang CR, Schneider AM, Lu Y, Niranjan T, Shen P, Robinson MA, et al. Mobile interspersed
21 repeats are major structural variants in the human genome. Cell. 2010;141(7):1171-82. Epub
22 2010/07/07. doi: 10.1016/j.cell.2010.05.026. PubMed PMID: 20602999; PubMed Central PMCID:
23 PMCPMC2943426.
24 60.   Treiber CD, Waddell S. Resolving the prevalence of somatic transposition in Drosophila. eLife.
25 2017;6. doi: 10.7554/eLife.28297. PubMed PMID: 28742021; PubMed Central PMCID:
26 PMCPMC5553932.
27 61.   Zhuang J, Wang J, Theurkauf W, Weng Z. TEMP: a computational method for analyzing
28 transposable element polymorphism in populations. Nucleic acids research. 2014;42(11):6826-38. doi:
29 10.1093/nar/gku323. PubMed PMID: 24753423; PubMed Central PMCID: PMC4066757.
30 62.   Perrat PN, DasGupta S, Wang J, Theurkauf W, Weng Z, Rosbash M, et al. Transposition-driven
31 genomic heterogeneity in the Drosophila brain. Science. 2013;340(6128):91-5. doi:
32 10.1126/science.1231965. PubMed PMID: 23559253; PubMed Central PMCID: PMC3887341.
33 63.   Khurana JS, Wang J, Xu J, Koppetsch BS, Thomson TC, Nowosielska A, et al. Adaptation to P
34 element transposon invasion in Drosophila melanogaster. Cell. 2011;147(7):1551-63. Epub 2011/12/27.
35 doi: S0092-8674(11)01436-X [pii]

36 10.1016/j.cell.2011.11.042. PubMed PMID: 22196730; PubMed Central PMCID: PMC3246748.
37 64.   Sytnikova YA, Rahman R, Chirn GW, Clark JP, Lau NC. Transposable element dynamics and PIWI
38 regulation impacts lncRNA and gene expression diversity in Drosophila ovarian cell cultures. Genome
39 research. 2014;24(12):1977-90. doi: 10.1101/gr.178129.114. PubMed PMID: 25267525; PubMed Central
40 PMCID: PMC4248314.
41 65.   Rahman R, Chirn GW, Kanodia A, Sytnikova YA, Brembs B, Bergman CM, et al. Unique
42 transposon landscapes are pervasive across Drosophila melanogaster genomes. Nucleic acids research.
43 2015;43(22):10655-72. doi: 10.1093/nar/gkv1193. PubMed PMID: 26578579; PubMed Central PMCID:
44 PMCPMC4678822.
45 66.   Penke TJ, McKay DJ, Strahl BD, Matera AG, Duronio RJ. Direct interrogation of the role of H3K9
46 in metazoan heterochromatin function. Genes & development. 2016;30(16):1866-80. Epub 2016/08/28.
47 doi: 10.1101/gad.286278.116. PubMed PMID: 27566777; PubMed Central PMCID: PMCPMC5024684.

1   67.   Ninova M, Chen YA, Godneeva B, Rogers AK, Luo Y, Fejes Toth K, et al. Su(var)2-10 and the
2   SUMO Pathway Link piRNA-Guided Target Recognition to Chromatin Silencing. Molecular cell.
3   2020;77(3):556-70 e6. Epub 2020/01/07. doi: 10.1016/j.molcel.2019.11.012. PubMed PMID: 31901446;
4   PubMed Central PMCID: PMCPMC7007863.
5   68.   Miller DE, Smith CB, Kazemi NY, Cockrell AJ, Arvanitakas AV, Blumenstiel JP, et al. Whole-
6   Genome Analysis of Individual Meiotic Events in Drosophila melanogaster Reveals That Noncrossover
7   Gene Conversions Are Insensitive to Interference and the Centromere Effect. Genetics. 2016;203(1):159-
8   71. doi: 10.1534/genetics.115.186486. PubMed PMID: 26944917; PubMed Central PMCID:
9   PMCPMC4858771.
10 69.   mod EC, Roy S, Ernst J, Kharchenko PV, Kheradpour P, Negre N, et al. Identification of functional
11 elements and regulatory circuits by Drosophila modENCODE. Science. 2010;330(6012):1787-97. doi:
12 10.1126/science.1198374. PubMed PMID: 21177974; PubMed Central PMCID: PMC3192495.
13 70.   Rubin GM, Hong L, Brokstein P, Evans-Holm M, Frise E, Stapleton M, et al. A Drosophila
14 complementary DNA resource. Science. 2000;287(5461):2222-4. Epub 2000/03/24. doi:
15 10.1126/science.287.5461.2222. PubMed PMID: 10731138.
16 71.   Li W, Jin Y, Prazak L, Hammell M, Dubnau J. Transposable elements in TDP-43-mediated
17 neurodegenerative disorders. PloS one. 2012;7(9):e44099. doi: 10.1371/journal.pone.0044099. PubMed
18 PMID: 22957047; PubMed Central PMCID: PMCPMC3434193.
19 72.   Brown EJ, Nguyen AH, Bachtrog D. The Y chromosome may contribute to sex-specific ageing in
20 Drosophila. Nat Ecol Evol. 2020;4(6):853-62. Epub 2020/04/22. doi: 10.1038/s41559-020-1179-5.
21 PubMed PMID: 32313175; PubMed Central PMCID: PMCPMC7274899.
22 73.   Srivastav SP, Rahman R, Ma Q, Pierre J, Bandyopadhyay S, Lau NC. Har-P, a short P-element
23 variant, weaponizes P-transposase to severely impair Drosophila development. eLife. 2019;8. doi:
24 10.7554/eLife.49948. PubMed PMID: 31845649; PubMed Central PMCID: PMCPMC6917496.
25 74.   Wang L, Dou K, Moon S, Tan FJ, Zhang ZZ. Hijacking Oogenesis Enables Massive Propagation of
26 LINE and Retroviral Transposons. Cell. 2018;174(5):1082-94 e12. doi: 10.1016/j.cell.2018.06.040.
27 PubMed PMID: 30057117.
28 75.   Okamura K, Balla S, Martin R, Liu N, Lai EC. Two distinct mechanisms generate endogenous
29 siRNAs from bidirectional transcription in Drosophila melanogaster. Nat Struct Mol Biol. 2008;15(9):998.
30 Epub 2008/09/05. doi: nsmb0908-998c [pii]

31 10.1038/nsmb0908-998c. PubMed PMID: 18769470.
32 76.   Kawamura Y, Saito K, Kin T, Ono Y, Asai K, Sunohara T, et al. Drosophila endogenous small RNAs
33 bind to Argonaute 2 in somatic cells. Nature. 2008;453(7196):793-7. Epub 2008/05/09. doi: nature06938
34 [pii]

35 10.1038/nature06938. PubMed PMID: 18463636.
36 77.   Czech B, Malone CD, Zhou R, Stark A, Schlingeheyde C, Dus M, et al. An endogenous small
37 interfering RNA pathway in Drosophila. Nature. 2008;453(7196):798-802. PubMed PMID: 18463631.
38 78.   Brennecke J, Aravin AA, Stark A, Dus M, Kellis M, Sachidanandam R, et al. Discrete small RNA-
39 generating loci as master regulators of transposon activity in Drosophila. Cell. 2007;128(6):1089-103.
40 Epub 2007/03/10. doi: S0092-8674(07)00257-7 [pii]

41 10.1016/j.cell.2007.01.043. PubMed PMID: 17346786.
42 79.   Saito K, Nishida KM, Mori T, Kawamura Y, Miyoshi K, Nagami T, et al. Specific association of Piwi
43 with rasiRNAs derived from retrotransposon and heterochromatic regions in the Drosophila genome.
44 Genes & development. 2006;20(16):2214-22. Epub 2006/08/03. doi: gad.1454806 [pii]

45 10.1101/gad.1454806. PubMed PMID: 16882972; PubMed Central PMCID: PMC1553205.

80. Vagin VV, Sigova A, Li C, Seitz H, Gvozdev V, Zamore PD. A distinct small RNA pathway silences selfish genetic elements in the germline. Science. 2006;313(5785):320-4. PubMed PMID: 16809489.

81. Moller HD, Mohiyuddin M, Prada-Luengo I, Sailani MR, Halling JF, Plomgaard P, et al. Circular DNA elements of chromosomal origin are common in healthy human somatic tissue. Nature communications. 2018;9(1):1069. doi: 10.1038/s41467-018-03369-8. PubMed PMID: 29540679; PubMed Central PMCID: PMCPMC5852086.

82. Shmookler Reis RJ, Lumpkin CK, Jr., McGill JR, Riabowol KT, Goldstein S. Genome alteration during in vitro and in vivo aging: amplification of extrachromosomal circular DNA molecules containing a chromosomal sequence of variable repeat frequency. Cold Spring Harbor symposia on quantitative biology. 1983;47 Pt 2:1135-9. PubMed PMID: 6574863.

83. Shibata Y, Kumar P, Layer R, Willcox S, Gagan JR, Griffith JD, et al. Extrachromosomal microDNAs and chromosomal microdeletions in normal tissues. Science. 2012;336(6077):82-6. doi: 10.1126/science.1213307. PubMed PMID: 22403181; PubMed Central PMCID: PMCPMC3703515.

84. Misra R, Shih A, Rush M, Wong E, Schmid CW. Cloned extrachromosomal circular DNA copies of the human transposable element THE-1 are related predominantly to a single type of family member. J Mol Biol. 1987;196(2):233-43. PubMed PMID: 2821286.

85. Turner KM, Deshpande V, Beyter D, Koga T, Rusert J, Lee C, et al. Extrachromosomal oncogene amplification drives tumour evolution and genetic heterogeneity. Nature. 2017;543(7643):122-5. doi: 10.1038/nature21356. PubMed PMID: 28178237; PubMed Central PMCID: PMCPMC5334176.

86. Dillon LW, Kumar P, Shibata Y, Wang YH, Willcox S, Griffith JD, et al. Production of Extrachromosomal MicroDNAs Is Linked to Mismatch Repair Pathways and Transcriptional Activity. Cell reports. 2015;11(11):1749-59. doi: 10.1016/j.celrep.2015.05.020. PubMed PMID: 26051933; PubMed Central PMCID: PMCPMC4481157.

87. Vu W, Nuzhdin S. Genetic variation of copia suppression in Drosophila melanogaster. Heredity (Edinb). 2011;106(2):207-17. doi: 10.1038/hdy.2010.41. PubMed PMID: 20606692; PubMed Central PMCID: PMCPMC3183883.

88. Flavell AJ, Ish-Horowicz D. Extrachromosomal circular copies of the eukaryotic transposable element copia in cultured Drosophila cells. Nature. 1981;292(5824):591-5. PubMed PMID: 6265802.

89. Cohen S, Yacobi K, Segal D. Extrachromosomal circular DNA of tandemly repeated genomic sequences in Drosophila. Genome research. 2003;13(6A):1133-45. doi: 10.1101/gr.907603. PubMed PMID: 12799349; PubMed Central PMCID: PMCPMC403641.

90. Mossie KG, Young MW, Varmus HE. Extrachromosomal DNA forms of copia-like transposable elements, F elements and middle repetitive DNA sequences in Drosophila melanogaster. Variation in cultured cells and embryos. J Mol Biol. 1985;182(1):31-43. PubMed PMID: 2582138.

91. Ilyin YV, Schuppe NG, Lyubomirskaya NV, Gorelova TV, Arkhipova IR. Circular copies of mobile dispersed genetic elements in cultured Drosophila melanogaster cells. Nucleic acids research. 1984;12(19):7517-31. PubMed PMID: 6093043; PubMed Central PMCID: PMCPMC320178.

92. Lanciano S, Carpentier MC, Llauro C, Jobet E, Robakowska-Hyzorek D, Lasserre E, et al. Sequencing the extrachromosomal circular mobilome reveals retrotransposon activity in plants. PLoS genetics. 2017;13(2):e1006630. doi: 10.1371/journal.pgen.1006630. PubMed PMID: 28212378; PubMed Central PMCID: PMCPMC5338827.

93. Chinen M, Lei EP. Drosophila Argonaute2 turnover is regulated by the ubiquitin proteasome pathway. Biochem Biophys Res Commun. 2017;483(3):951-7. Epub 2017/01/15. doi: 10.1016/j.bbrc.2017.01.039. PubMed PMID: 28087276; PubMed Central PMCID: PMCPMC5279065.

94. Lewis A, Berkyurek AC, Greiner A, Sawh AN, Vashisht A, Merrett S, et al. A Family of Argonaute-Interacting Proteins Gates Nuclear RNAi. Molecular cell. 2020;78(5):862-75 e8. Epub 2020/04/30. doi: 10.1016/j.molcel.2020.04.007. PubMed PMID: 32348780.

95.   Clark JP, Rahman R, Yang N, Yang LH, Lau NC. Drosophila PAF1 Modulates PIWI/piRNA Silencing Capacity. Curr Biol. 2017;27(17):2718-26 e4. doi: 10.1016/j.cub.2017.07.052. PubMed PMID: 28844648; PubMed Central PMCID: PMCPMC5611886.

96.   Kowalik KM, Shimada Y, Flury V, Stadler MB, Batki J, Buhler M. The Paf1 complex represses small-RNA-mediated epigenetic gene silencing. Nature. 2015;520(7546):248-52. doi: 10.1038/nature14337. PubMed PMID: 25807481; PubMed Central PMCID: PMCPMC4398878.

97.   Yamanaka S, Mehta S, Reyes-Turcu FE, Zhuang F, Fuchs RT, Rong Y, et al. RNAi triggered by specialized machinery silences developmental genes and retrotransposons. Nature. 2013;493(7433):557-60. doi: 10.1038/nature11716. PubMed PMID: 23151475; PubMed Central PMCID: PMC3554839.

98.   Pfeiffer BD, Ngo TT, Hibbard KL, Murphy C, Jenett A, Truman JW, et al. Refinement of tools for targeted gene expression in Drosophila. Genetics. 2010;186(2):735-55. doi: 10.1534/genetics.110.119917. PubMed PMID: 20697123; PubMed Central PMCID: PMCPMC2942869.

99.   Fast I, Rosenkranz D. Temperature-dependent small RNA expression in Drosophila melanogaster. RNA biology. 2018;15(3):308-13. Epub 2018/01/19. doi: 10.1080/15476286.2018.1429881. PubMed PMID: 29345184; PubMed Central PMCID: PMCPMC5927726.

100.   Kelleher ES, Jaweria J, Akoma U, Ortega L, Tang W. QTL mapping of natural variation reveals that the developmental regulator bruno reduces tolerance to P-element transposition in the Drosophila female germline. PLoS biology. 2018;16(10):e2006040. doi: 10.1371/journal.pbio.2006040. PubMed PMID: 30376574; PubMed Central PMCID: PMCPMC6207299.

101.   Moon S, Cassani M, Lin YA, Wang L, Dou K, Zhang ZZ. A Robust Transposon-Endogenizing Response from Germline Stem Cells. Developmental cell. 2018;47(5):660-71 e3. doi: 10.1016/j.devcel.2018.10.011. PubMed PMID: 30393075.

102.   Genenncher B, Durdevic Z, Hanna K, Zinkl D, Mobin MB, Senturk N, et al. Mutations in Cytosine-5 tRNA Methyltransferases Impact Mobile Element Expression and Genome Stability at Specific DNA Repeats. Cell reports. 2018;22(7):1861-74. Epub 2018/02/15. doi: 10.1016/j.celrep.2018.01.061. PubMed PMID: 29444437.

103.   Robinow S, White K. The locus elav of Drosophila melanogaster is expressed in neurons at all developmental stages. Developmental biology. 1988;126(2):294-303. Epub 1988/04/01. doi: 10.1016/0012-1606(88)90139-x. PubMed PMID: 3127258.

104.   Amarasinghe SL, Su S, Dong X, Zappia L, Ritchie ME, Gouil Q. Opportunities and challenges in long-read sequencing data analysis. Genome biology. 2020;21(1):30. Epub 2020/02/09. doi: 10.1186/s13059-020-1935-5. PubMed PMID: 32033565; PubMed Central PMCID: PMCPMC7006217.

105.   Lee YS, Nakahara K, Pham JW, Kim K, He Z, Sontheimer EJ, et al. Distinct roles for Drosophila Dicer-1 and Dicer-2 in the siRNA/miRNA silencing pathways. Cell. 2004;117(1):69-81. Epub 2004/04/07. doi: S0092867404002612 [pii]. PubMed PMID: 15066283.

106.   Senti KA, Jurczak D, Sachidanandam R, Brennecke J. piRNA-guided slicing of transposon transcripts enforces their transcriptional silencing via specifying the nuclear piRNA repertoire. Genes & development. 2015;29(16):1747-62. doi: 10.1101/gad.267252.115. PubMed PMID: 26302790; PubMed Central PMCID: PMCPMC4561483.

107.   Belancio VP, Roy-Engel AM, Pochampally RR, Deininger P. Somatic expression of LINE-1 elements in human tissues. Nucleic acids research. 2010;38(12):3909-22. Epub 2010/03/11. doi: 10.1093/nar/gkq132. PubMed PMID: 20215437; PubMed Central PMCID: PMCPMC2896524.

108.   Mumford PW, Romero MA, Osburn SC, Roberson PA, Vann CG, Mobley CB, et al. Skeletal muscle LINE-1 retrotransposon activity is upregulated in older versus younger rats. Am J Physiol Regul Integr Comp Physiol. 2019;317(3):R397-R406. Epub 2019/06/13. doi: 10.1152/ajpregu.00110.2019. PubMed PMID: 31188650.

109.   Romero MA, Mumford PW, Roberson PA, Osburn SC, Parry HA, Kavazis AN, et al. Five months of voluntary wheel running downregulates skeletal muscle LINE-1 gene expression in rats. Am J Physiol Cell Physiol. 2019;317(6):C1313-C23. Epub 2019/10/17. doi: 10.1152/ajpcell.00301.2019. PubMed PMID: 31618076.

110.   Nandakumar S, Grushko O, Buttitta LA. Polyploidy in the adult Drosophila brain. eLife. 2020;9. Epub 2020/08/26. doi: 10.7554/eLife.54385. PubMed PMID: 32840209; PubMed Central PMCID: PMCPMC7447450.

111.   Yarosh W, Spradling AC. Incomplete replication generates somatic DNA alterations within Drosophila polytene salivary gland cells. Genes & development. 2014;28(16):1840-55. doi: 10.1101/gad.245811.114. PubMed PMID: 25128500; PubMed Central PMCID: PMC4197960.

112.   Vienne J, Spann R, Guo F, Rosbash M. Age-Related Reduction of Recovery Sleep and Arousal Threshold in Drosophila. Sleep. 2016;39(8):1613-24. Epub 2016/06/17. doi: 10.5665/sleep.6032. PubMed PMID: 27306274; PubMed Central PMCID: PMCPMC4945321.

113.   Ren X, Yang Z, Mao D, Chang Z, Qiao HH, Wang X, et al. Performance of the Cas9 nickase system in Drosophila melanogaster. G3 (Bethesda). 2014;4(10):1955-62. Epub 2014/08/17. doi: 10.1534/g3.114.013821. PubMed PMID: 25128437; PubMed Central PMCID: PMCPMC4199701.

114.   Lee SK, Xue Y, Shen W, Zhang Y, Joo Y, Ahmad M, et al. Topoisomerase 3beta interacts with RNAi machinery to promote heterochromatin formation and transcriptional silencing in Drosophila. Nature communications. 2018;9(1):4946. Epub 2018/11/25. doi: 10.1038/s41467-018-07101-4. PubMed PMID: 30470739; PubMed Central PMCID: PMCPMC6251927.

115.   Nazer E, Dale RK, Chinen M, Radmanesh B, Lei EP. Argonaute2 and LaminB modulate gene expression by controlling chromatin topology. PLoS genetics. 2018;14(3):e1007276. Epub 2018/03/13. doi: 10.1371/journal.pgen.1007276. PubMed PMID: 29529026; PubMed Central PMCID: PMCPMC5864089.

116.   Hain D, Bettencourt BR, Okamura K, Csorba T, Meyer W, Jin Z, et al. Natural variation of the amino-terminal glutamine-rich domain in Drosophila argonaute2 is not associated with developmental defects. PloS one. 2010;5(12):e15264. doi: 10.1371/journal.pone.0015264. PubMed PMID: 21253006; PubMed Central PMCID: PMC3002974.

117.   Zamparini AL, Davis MY, Malone CD, Vieira E, Zavadil J, Sachidanandam R, et al. Vreteno, a gonad-specific protein, is essential for germline development and primary piRNA biogenesis in Drosophila. Development. 2011;138(18):4039-50. Epub 2011/08/13. doi: dev.069187 [pii]

10.1242/dev.069187. PubMed PMID: 21831924; PubMed Central PMCID: PMC3160098.

118.   Shang Y, Griffith LC, Rosbash M. Light-arousal and circadian photoreception circuits intersect at the large PDF cells of the Drosophila brain. Proceedings of the National Academy of Sciences of the United States of America. 2008;105(50):19587-94. doi: 10.1073/pnas.0809577105. PubMed PMID: 19060186; PubMed Central PMCID: PMC2596742.

119.   Nagoshi E, Sugino K, Kula E, Okazaki E, Tachibana T, Nelson S, et al. Dissecting differential gene expression within the circadian neuronal circuit of Drosophila. Nature neuroscience. 2010;13(1):60-8. Epub 2009/12/08. doi: 10.1038/nn.2451. PubMed PMID: 19966839; PubMed Central PMCID: PMCPMC3878269.

120.   Chirn GW, Rahman R, Sytnikova YA, Matts JA, Zeng M, Gerlach D, et al. Conserved piRNA Expression from a Distinct Set of piRNA Cluster Loci in Eutherian Mammals. PLoS genetics. 2015;11(11):e1005652. doi: 10.1371/journal.pgen.1005652. PubMed PMID: 26588211; PubMed Central PMCID: PMCPMC4654475.

121.   Li H, Durbin R. Fast and accurate long-read alignment with Burrows-Wheeler transform. Bioinformatics. 2010;26(5):589-95. doi: 10.1093/bioinformatics/btp698. PubMed PMID: 20080505; PubMed Central PMCID: PMC2828108.

1   122.   Langmead B, Trapnell C, Pop M, Salzberg SL. Ultrafast and memory-efficient alignment of short
2   DNA sequences to the human genome. Genome biology. 2009;10(3):R25. doi: 10.1186/gb-2009-10-3-
3   r25. PubMed PMID: 19261174; PubMed Central PMCID: PMC2690996.

4

5

6

1   **FIGURE LEGENDS**

2

3   **Figure 1. Overview of study to examine whether TE-DNA copy numbers change**

4   **during fly aging.**

5   (A) Survival curves of the three wild-type fly strains carried out in this study, indicating

6   the selection of 30-day adults as a representative timepoint of aging onset. (B)

7   Validation of TE transcript expression increases during fly aging through qRT-PCR of

8   TE RNAs normalized to *rp49* transcripts. Error bars are propagated standard deviations

9   of delta-CT values from three replicates. (C) Overview of TE detection strategy from

10   Whole Genome Sequencing (WGS) data using updated TIDAL-Fly and extra-

11   chromosomal circular DNA (eccDNAs) detection scripts. (D) Study designed for

12   comparing TE load between 5-day young and 30-day aged flies within each wild-type

13   and mutant strain.

14

15   **Figure 2. WGS analysis of TE insertion numbers between 5-day young versus 30-**

16   **day aged wild-type fly strains.**

17   (A) Quantification of new TE insertions as compared to the reference genome using the

18   TIDAL-fly program. Categories of total TE insertions broken by the Coverage Ratios

19   (CR) of CR>2 and CR<=2. (B) Within each strain, TE families' percentages are ordered

20   by the color legend. (C) Ratios of the 30-day versus 5-day of normalized TE insertions

21   from panels D-F. Note the *w1118* strain has the greatest number of distinct TE

22   insertions detected by TIDAL. (D-F) Number of unique TE insertions (filled bars) present

23   in 5-day and 30-day relative to common insertions present in both samples (open bar)

24   of *w1118, OreR* and *ISO1* fly strains. These panels display only the TE families that

36

1   were detected by TIDAL be at least 1% of total number of TE families (*i.e.* all the TEs

2   not lumped into the "Others" category of Fig. 2B).

3

4   **Figure 3. WGS analysis of TE insertion numbers between Young (5-day) versus**

5   **Aged (30-day) RNAi mutants fly strains.**

6   (A-C) Quantification of new TE insertions as compared to the reference genome using

7   the TIDAL-fly program. Categories of total TE insertions broken by the coverage ratios

8   (CR) of CR>2 and CR<=2. Dashed arrows highlight the accumulation of TE insertions in

9   a single generation of aging in two distinct strains of each RNAi null mutants in *piwi-/-,*

10   *aub-/-, and AGO2-/-* genes. (D-F) Ratios of the 30-day versus 5-day of normalized TE

11   insertions from panels A-C. These panels display only the TE families that were

12   detected by TIDAL be at least 1% of total number of TE families (*i.e.* all the TEs not

13   lumped into the "Others" category of Fig. 2B).

14

15   **Figure 4. Aging-associated TE landscape changes in fly brains of WT and RNAi**

16   **mutant strains.**

17   (A) Validation of fly brain dissections by microscopy and RT-PCR of brain-specific gene

18   expression. TIDAL analysis of WGS for new TE insertions in the brains of (B) Wild-type

19   (WT) strains, (C) *piwi* mutants, and (D) *Ago2* mutants. The bar graphs on the left

20   represent categories of total TE insertions broken by the Coverage Ratios (CR) of CR>2

21   and CR<=2. Dashed arrows highlight the accumulation of TE insertions in a single

22   generation of aging flies. The dot graphs to the right show the ratios of the 30-day

23   versus 5-day of normalized TE insertions from left panels B-D. These panels display

1   only the TE families that were detected by TIDAL be at least 1% of total number of TE

2   families, hence only three blue dots for ISO1 are visible in (B).

3

4   **Figure 5. Aging *Drosophila* display increases in TEs existing as extra-**

5   **chromosomal circular DNA (eccDNA).**

6   (A) Diagram of methodology to enrich and purify eccDNAs for direct library construction

7   and sequencing without requiring prior amplification. (B) Genomic PCR from WT flies

8   demonstrating the depletion of linear gDNA and enrichment of eccDNA with TE

9   sequences during exonucleases treatments. Inset diagram explains configuration of

10   PCR primers. Left diagram explains configuration of PCR primers, L=DNA ladder. (C)

11   qPCR validation of spike-in plasmids and *copia* eccDNA after exonucleases treatments

12   of *ISO1* gDNA from young versus aged adult flies. (D) Ratio of the read coverage just

13   across the *copia* consensus sequence comparing young versus aged flies. (E) Box plots

14   of 30-day/5-day ratios of read coverage for eccDNA TE sequences rated by the

15   CIRCLE-Map pipeline with significant "circle score" >50 (Moller et al, 2018); and for our

16   own custom quantitation pipeline that uses a TE-mapping scripts previously used for

17   small RNA analysis. (F) Dot graphs highlighting specific TE eccDNAs whose 30-day/5-

18   day sequencing ratios are normalized to the RPM library size or further normalized to

19   the plasmid spike-ins from (E). These panels display only the TE families that had

20   "circle score" >50 (left) or displayed a measurable 30-day/5-day ratio from the custom

21   analysis pipeline (right).

22

23   **Figure 6. Genetic interventions of TE expression in adult *Drosophila*.**

1   (A) Overexpressing AGO2 [Tub>Gal4;UAS-HA-*AGO2*]/[Tub>Gal4] and (B)

2   overexpressing PIWI [Tub>Gal4;UAS-3X-HA *piwi*]/[Tub>Gal4] results in a reduction of

3   TE RNA expression in 5-day young adult *Drosophila*. Left graphs confirm gene

4   overexpression and right graphs detail TE RNA expression measured by RT-qPCR of

5   the target gene compared to the *rp49* housekeeping gene and with error bars

6   representing propagated standard error of triplicate measurements. (C) Adult-specific

7   knockdown of *PAF1* in 5-day young females qualitatively assessed in the gel (left) and

8   RT-qPCR (middle), which reduces TE RNA expression (right). The genes *TFIIs* and *piwi*

9   are controls suggesting that TE RNA reduction is distinct from a concern that *PAF1*

10   RNAi would simply be causing global reduction in transcription. Examining the effect of

11   TE RNA reduction in the *PAF1* knockdown in the ovary (D) and brain (E) of adult

12   *Drosophila* with TEs and *PAF1* in left graph and control genes in the right graph. (F) Life

13   span comparison between control versus *PAF1* RNAi knockdown of adult female flies

14   upon raising them at 29 °C to release the GAL80^{ts} inhibitor to induce RNAi from the

15   Tub>GAL4. *PAF1 RNAi* n=112, Control RNAi n=170.

16

17

18

19   **SUPPORTING ONLINE MATERIALS LIST**

20   **Supplementary Text, Supplementary Figures and Tables legends.**

21   **Figures S1-S5.**

22   **Tables S1-S3.**

23

24
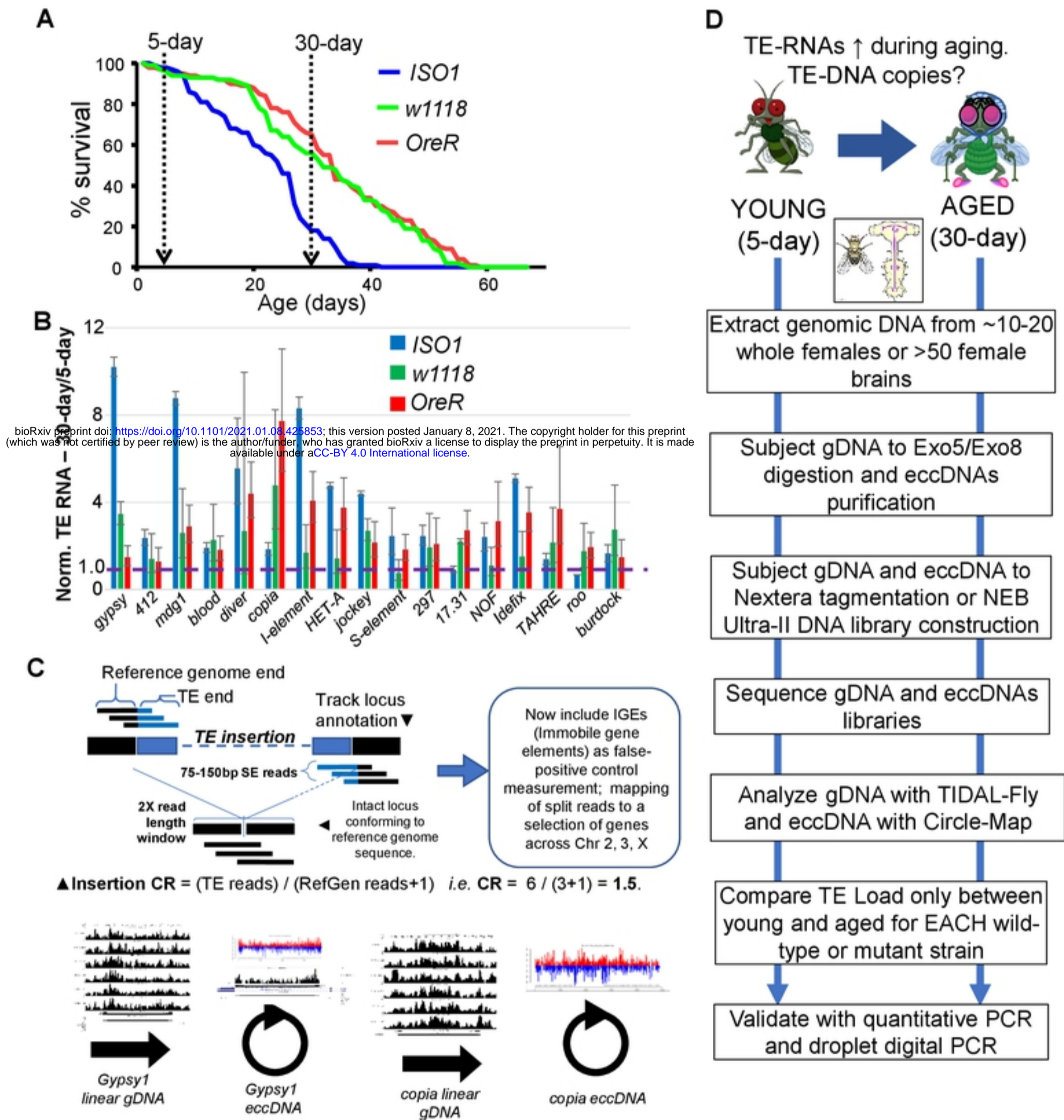
Figure 1. Overview of study to examine whether TE-DNA copy numbers change during fly aging.
(A) Survival curves of the three wild-type (WT) fly strains carried out in this study, indicating the selection of 30-day adults as a representative timepoint of aging onset. (B) Validation of TE transcript expression increases during fly aging through qRT-PCR of TE RNAs normalized to *rp49* transcripts. Error bars are propagated standard deviations of delta-CT values from three replicates. (C) Overview of TE detection strategy from Whole Genome Sequencing (WGS) data using updated TIDAL and extra-chromosomal circular DNA (eccDNAs) detection scripts. (D) Study designed for comparing TE load between 5-day young and 30-day aged flies within each WT and mutant strain.
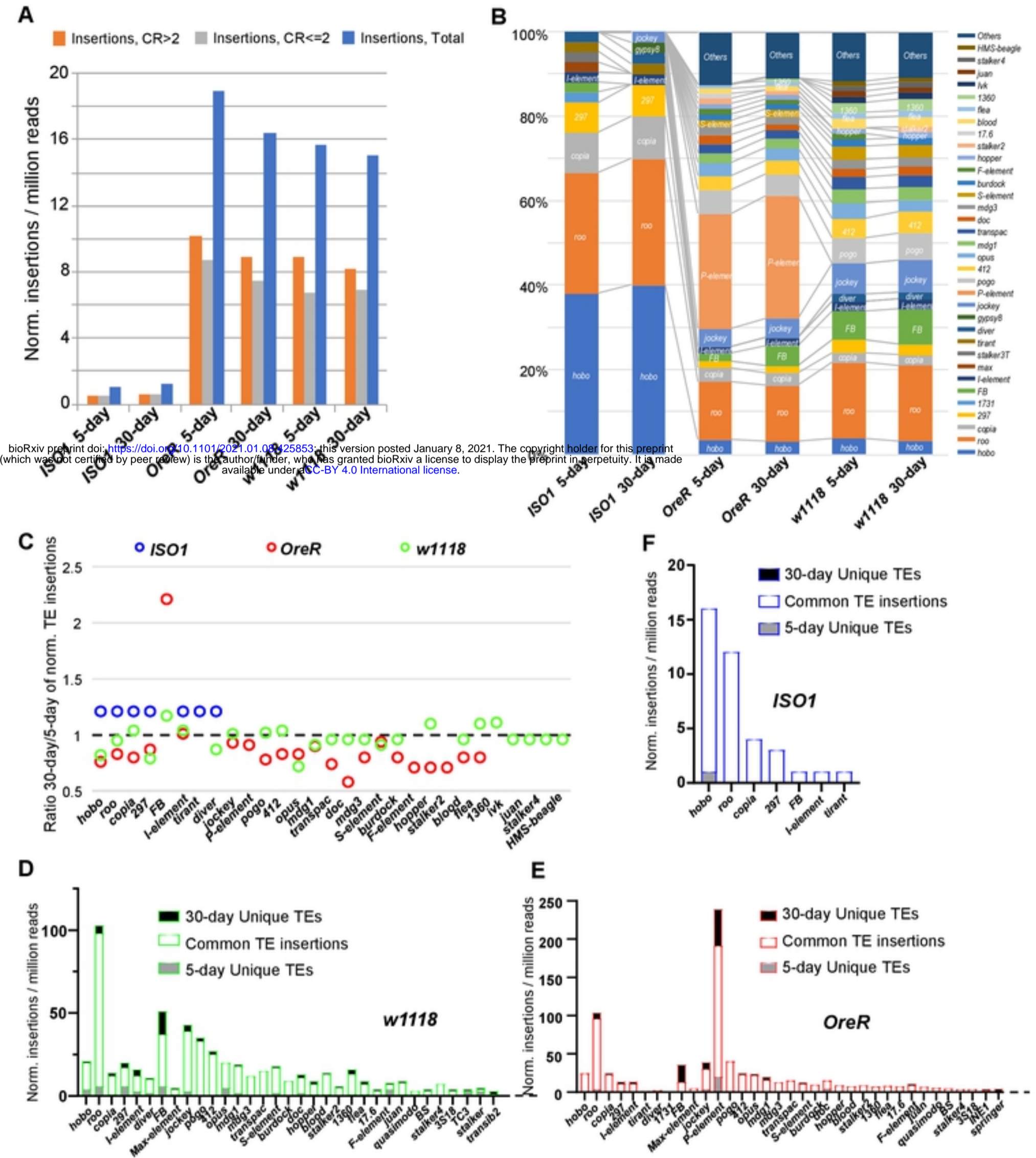
Figure 1

Figure 2. WGS analysis of TE insertion numbers between 5-day young versus 30-day aged wild-type fly strains.
(A) Quantification of new TE insertions as compared to the reference genome using the TIDAL program. Categories of total TE insertions broken by the Coverage Ratios (CR) of CR>2 and CR<=2. (B) Within each strain, TE families' percentages are ordered by the color legend. (C) Ratios of the 30-day versus 5-day of normalized TE insertions from panels D-F. Note the *w1118* strain has the greatest number of distinct TE insertions detected by TIDAL. (D-F) Number of unique TE insertions (filled bars) present in 5-day and 30-day relative to common insertions present in both samples (open bar) of *w1118, OreR* and *ISO1* fly strains. These panels display only the TE families that were detected by TIDAL be at least 1% of total number of TE families (*i.e.* all the TEs not lumped into the "Others" category of Fig. 2B).
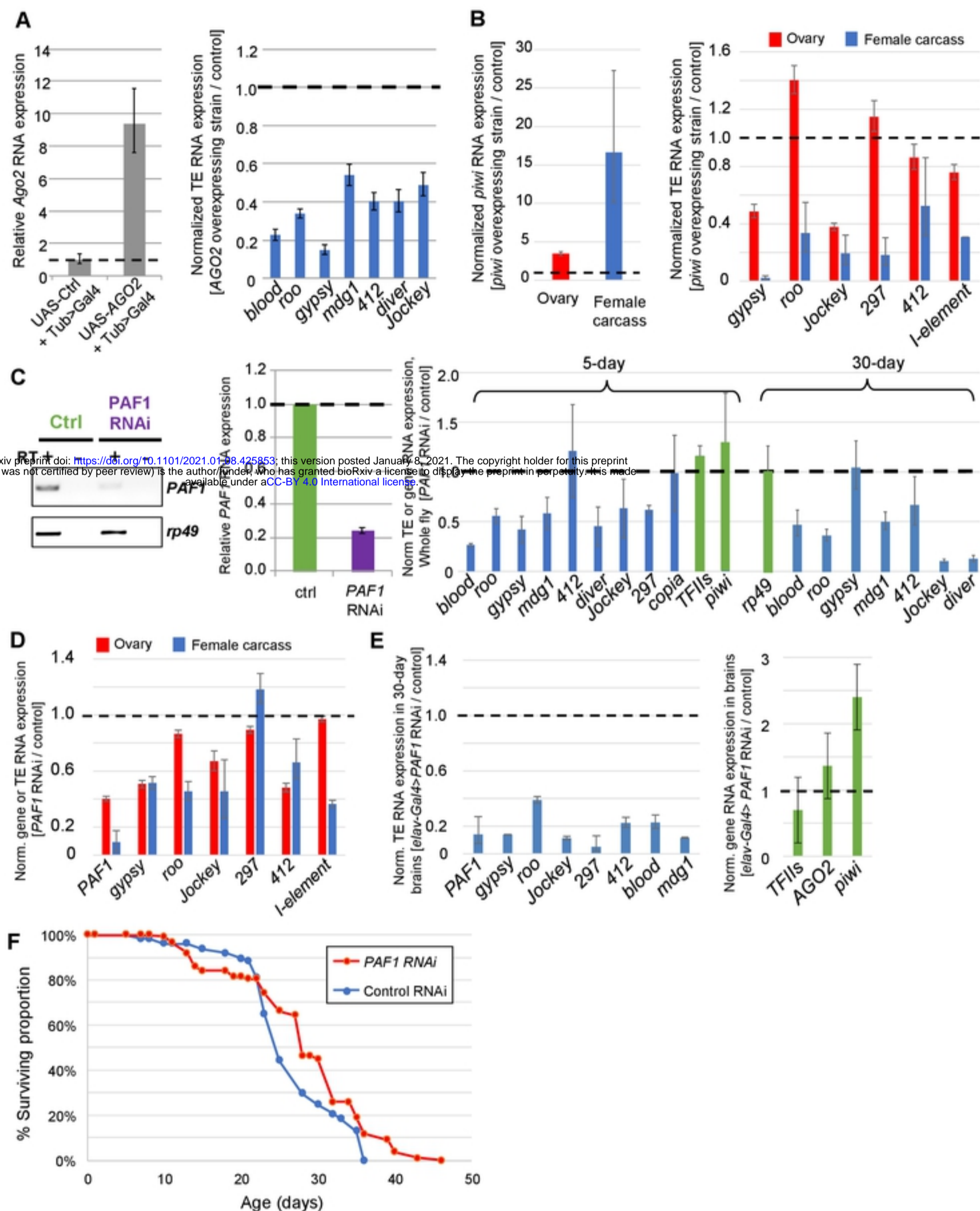
Figure 2

Figure 6. Genetic interventions of TE expression in adult _Drosophila_.
(A) Overexpressing AGO2 [Tub>Gal4;UAS-HA-_AGO2_]/[Tub>Gal4] and (B) overexpressing PIWI [Tub>Gal4;UAS-3X-HA _piwi_]/[Tub>Gal4] results in a reduction of TE RNA expression in 5-day young adult _Drosophila_. Left graphs confirm gene overexpression and right graphs detail TE RNA expression measured by RT-qPCR of the target gene compared to the _rp49_ housekeeping gene and with error bars representing propagated standard error of triplicate measurements. (C) Adult-specific knockdown of _PAF1_ in 5-day young females qualitatively assessed in the gel (left) and RT-qPCR (middle), which reduces TE RNA expression (right). The genes _TFIIs_ and _piwi_ are controls suggesting that TE RNA reduction is distinct from a concern that _PAF1_ RNAi would simply be causing global reduction in transcription. Examining the effect of TE RNA reduction in the PAF knockdown in the ovary (D) and brain (E) of adult _Drosophila_ with TEs and _PAF1_ in left graph and control genes in the right graph. (F) Life span comparison between control versus PAF1 RNAi knockdown of adult female flies upon raising them at 29 °C to release the GAL80^ts inhibitor to induce RNAi from the Tub>GAL4. _PAF1 RNAi_ n=112, Control RNAi n=170.
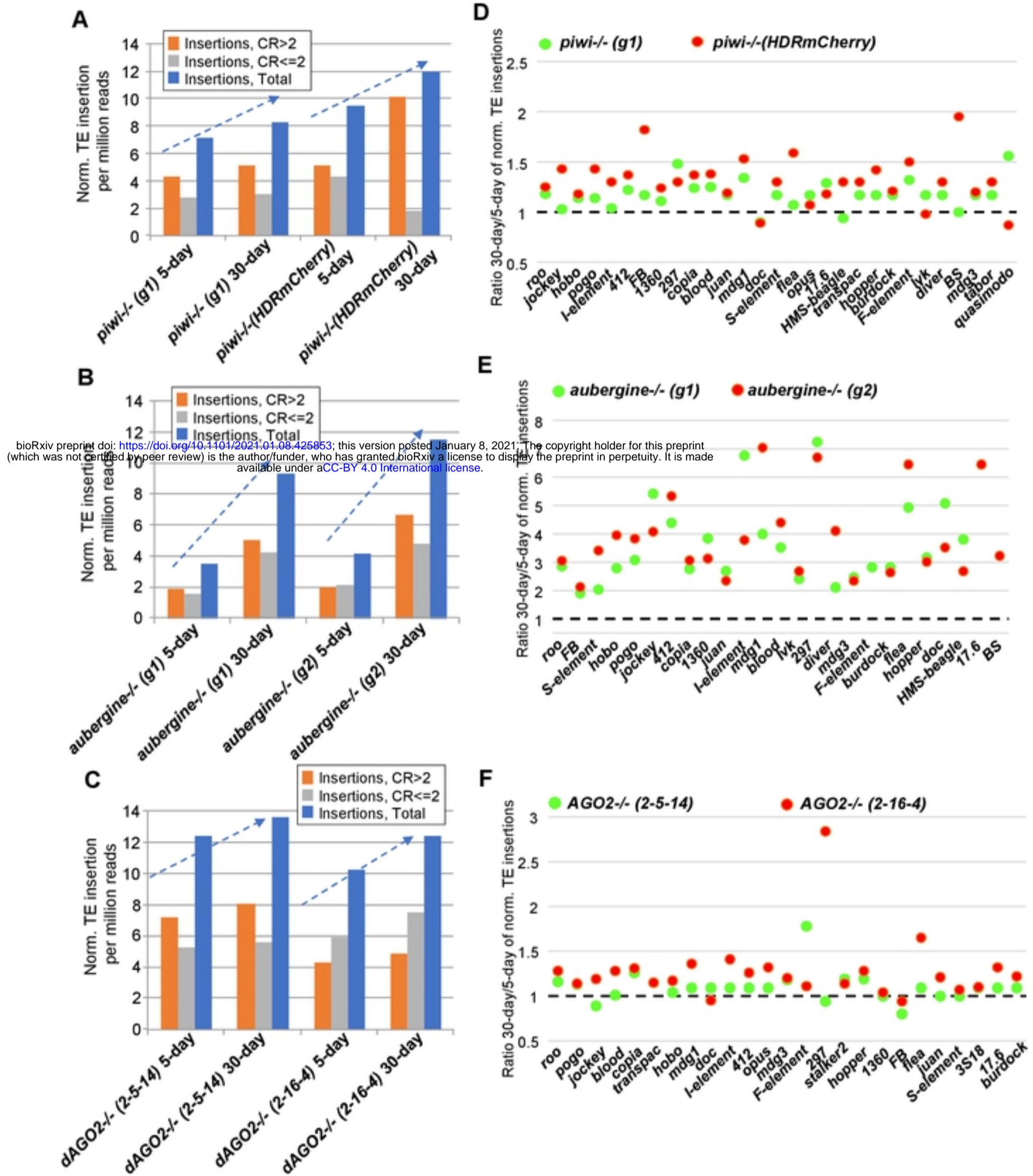
Figure 6

Figure 3. WGS analysis of TE insertion numbers between 5-day young versus 30-day aged RNAi mutant fly strains.
(A-C) Quantification of new TE insertions as compared to the reference genome using the TIDAL program. Categories of total TE insertions broken by the coverage ratios (CR) of CR>2 and CR<=2. Dashed arrows highlight the accumulation of TE insertions in a single generation of aging in two distinct strains of each RNAi null mutants in *piwi-/-, aub-/-, and AGO2-/-* genes. (D-F) Ratios of the 30-day versus 5-day of normalized TE insertions from panels A-C. These panels display only the TE families that were detected by TIDAL be at least 1% of total number of TE families (*i.e.* all the TEs not lumped into the "Others" category of Fig. 2B).

Figure 3
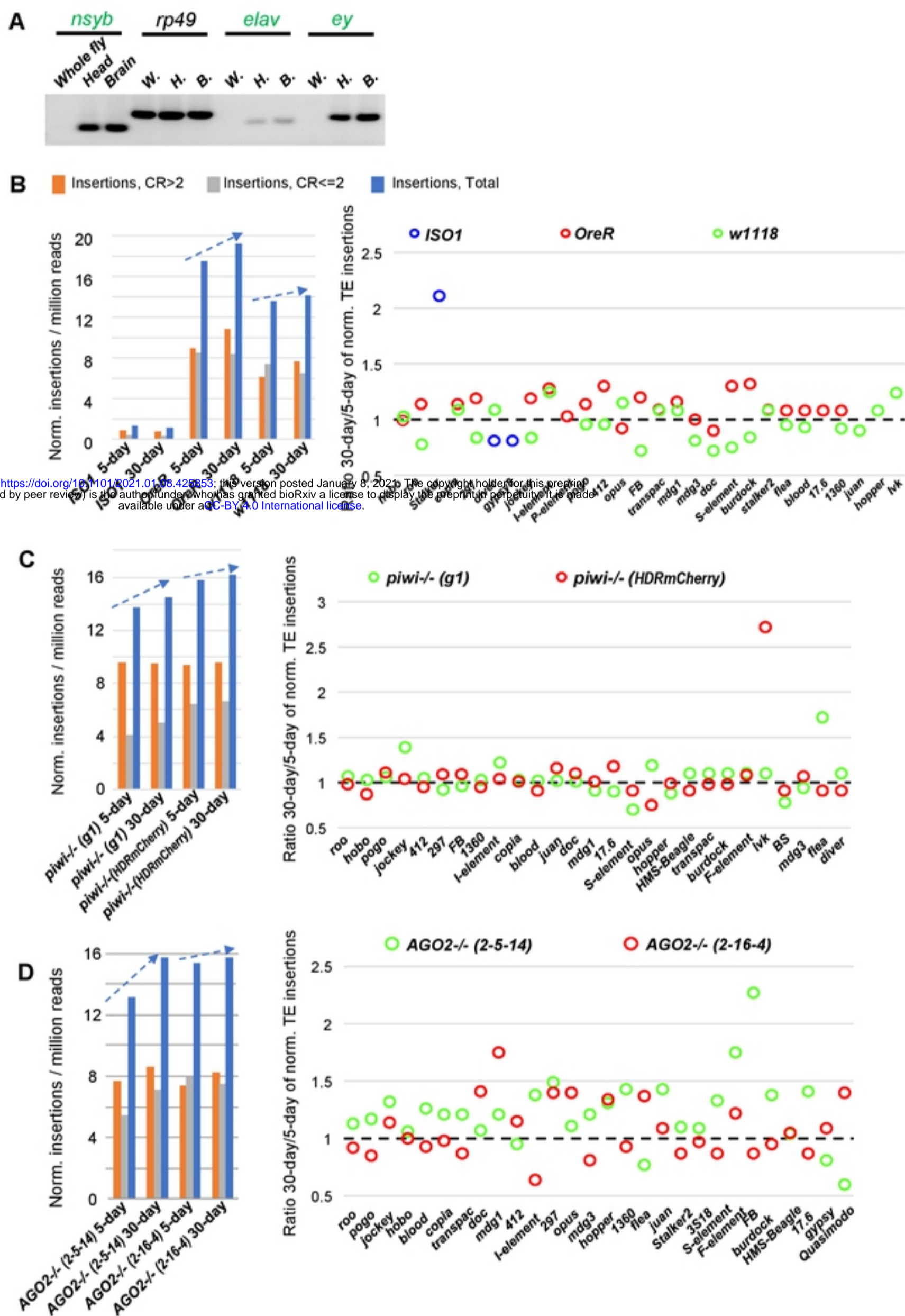
Figure 4. Aging-associated TE landscape changes in fly brains of WT and RNAi mutant strains.
(A) Validation of fly brain dissections by RT-PCR of brain-specific gene expression. TIDAL analysis of WGS for new TE insertions in the brains of (B) Wild-type (WT) strains, (C) *piwi* mutants, and (D) *Ago2* mutants. The bar graphs on the left represent categories of total TE insertions broken by the coverage ratios (CR) of CR>2 and CR<=2. Dashed arrows highlight the accumulation of TE insertions in a single generation of aging flies. The dot graphs to the right show the ratios of the 30-day versus 5-day of normalized TE insertions from left panels B-D. These panels display only the TE families that were detected by TIDAL be at least 1% of total number of TE families, hence only three blue dots for *ISO1* are visible in (B).
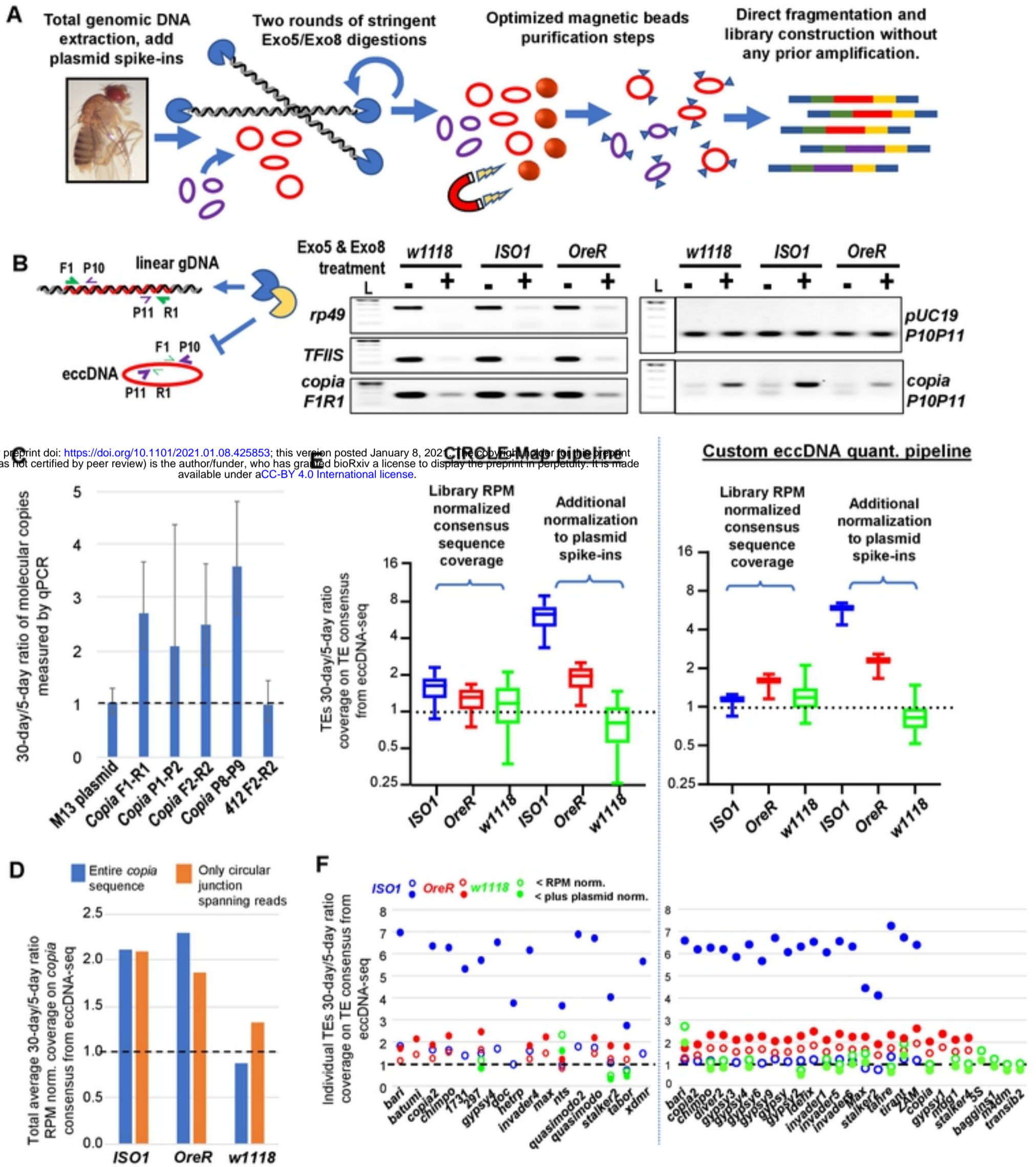
Figure 4

Figure 5. Aging *Drosophila* display increases in TEs existing as extra-chromosomal circular DNA (eccDNA).
(A) Diagram of methodology to enrich and purify eccDNAs for direct library construction and sequencing without requiring prior amplification.
(B) Genomic PCR from WT flies demonstrating the depletion of linear gDNA and enrichment of eccDNA with TE sequences during exonucleases treatments. Left diagram explains configuration of PCR primers, L=DNA ladder. (C) qPCR validation of spike-in plasmids and *copia* eccDNA after exonucleases treatments of *ISO1* gDNA from young versus aged adult flies. (D) Ratio of the read coverage just across the *copia* consensus sequence comparing young versus aged flies. (E) Box plots of 30-day/5-day ratios of read coverage for eccDNA TE sequences rated by the CIRCLE-Map pipeline with significant "circle score" >50 (Moller et al, 2018); and for our own custom quantitation pipeline that uses a TE-mapping scripts previously used for small RNA analysis. (F) Dot graphs highlighting specific TE eccDNAs whose 30-day/5-day sequencing ratios are normalized to the RPM library size or further normalized to the plasmid spike-ins from (E). These panels display only the TE families that had "circle score" >50 (left) or displayed a measurable 30-day/5-day ratio from the custom analysis pipeline (right).

Figure 5